Theory of Heusler and Full-Heusler compounds

Iosif Galanakis*

Department of Materials Science, School of Natural Sciences, University of Patras, GR-26504 Patra, Greece.

Abstract

Spintronics/magnetoelectronics brought at the center of scientific research the Heusler and full-Heusler compounds, since several among them have been shown to be half-metals. In this review we present a study of the basic electronic and magnetic properties of both Heusler families; the so-called semi-Heusler alloys like NiMnSb and the full-Heusler alloys like Co$_2$MnGe (usual full-Heuslers), Mn$_2$CoAl (inverse full-Heuslers) and (CoFe)MnAl (LiMgPdSn-type full-Heuslers). First-principles calculations are employed to discuss the origin of the gap which is fundamental for the understanding of their electronic and magnetic properties. For half-metallic Heusler compounds the total spin magnetic moment M_t scales linearly with the number of the valence electrons Z_t in the unit cell. These simple rules connect directly the magnetic to the electronic properties opening the way to engineer new half-metallic alloys with "à la carte" magnetic properties such as the quaternary half-metals, the so-called half-metallic antiferromagnets, magnetic semiconductors or even the more exotic spin-gapless semiconductors. Finally, special topics like exchange constants, defects, vacancies, surfaces and interfaces are being discussed.

---

*galanakis@upatras.gr

Theory of Heusler and Full-Heusler compounds

Iosif Galanakis (*galanakis@upatras.gr*)

Department of Materials Science, School of Natural Sciences,

University of Patras, GR-26504 Patra, Greece

Abstract

Spintronics/magnetoelectronics brought at the center of scientific research the Heusler and full-Heusler compounds, since several among them have been shown to be half-metals. In this review we present a study of the basic electronic and magnetic properties of both Heusler families; the so-called semi-Heusler alloys like NiMnSb and the full-Heusler alloys like Co_2MnGe (usual full-Heuslers), Mn_2CoAl (inverse full-Heuslers) and (CoFe)MnAl (LiMgPdSn-type full-Heuslers). First-principles calculations are employed to discuss the origin of the gap which is fundamental for the understanding of their electronic and magnetic properties. For half-metallic Heusler compounds the total spin magnetic moment M_t scales linearly with the number of the valence electrons Z_t in the unit cell. These simple rules connect directly the magnetic to the electronic properties opening the way to engineer new half-metallic alloys with "à la carte" magnetic properties such as the quaternary half-metals, the so-called half-metallic antiferromagnets, magnetic semiconductors or even the more exotic spin-gapless semiconductors. Finally, special topics like exchange constants, defects, vacancies, surfaces and interfaces are being discussed.

I. INTRODUCTION

Half-metallic magnets attracted the last two decades a lot of attention due to their possible applications in spintronics/magnetoelectronics [1, 2]. The addition of the spin degree of freedom to the conventional electronic devices based on semiconductors has several advantages like non-volatility, increased data processing speed, decreased electric power consumption and increased integration densities [3–5]. In the half-metallic materials the two spin bands show a completely different behavior. The majority spin band shows the typical metallic behavior, and the minority spin band exhibits a semiconducting behavior with a gap at the Fermi level. The existence of the gap leads to 100% spin-polarization at the Fermi level and thus a fully spinpolarised current should be feasible in these compounds maximizing the efficiency of magnetoelectronic devices [6, 7]. Bowen *et al.* have observed such a current in trilayers made up of half-metallic $La_{0.7}Sr_{0.3}MnO_3$ as electrodes and SrO_3 as a barrier [8].

The family of Heusler compounds, named after von Heusler [9], incorporates a huge number of magnetic members exhibiting diverse magnetic phenomena like itinerant and localized magnetism, antiferromagnetism, helimagnetism, Pauli paramagnetism or heavy-fermionic behavior [10–17]. The first Heusler alloys studied were crystallizing in the $L2_1$ structure which consists of 4 fcc sublattices (see figure 1). Afterwards, it was discovered that it is possible to leave one of the four sublattices unoccupied ($C1_b$ structure). The latter compounds are often called half- or semi-Heusler compounds or simply Heuslers, while the $L2_1$ compounds are known as full-Heusler compounds. The most-well known semi-Heusler compounds is NiMnSb [18]. In 1983 de Groot and his collaborators [19] showed using first-principles electronic structure calculations that this compound is in reality half-metallic, i.e. the minority band is semiconducting with a gap at the Fermi level E_F, leading to 100% spin polarization at E_F. Other known half-metallic materials except the semi- and full-Heusler alloys [20–24] are some oxides (*e.g* CrO_2 and Fe_3O_4) [25], the manganites (*e.g* $La_{0.7}Sr_{0.3}MnO_3$) [25], the double perovskites (*e.g.* Sr_2FeReO_6) [26], the pyrites (*e.g* CoS_2) [27], the transition metal chalcogenides (*e.g* CrSe) and pnictides (*e.g* CrAs) in the zinc-blende or wurtzite structures [28–51], the europium pnictides (*e.g* EuN) [52], the diluted magnetic semiconductors (*e.g* Mn impurities in Si or GaAs) [53, 54] and the so-called d^0 ferromagnets like CaAs [55]. Although thin films of CrO_2 and $La_{0.7}Sr_{0.3}MnO_3$ have been

verified to present practically 100% spin-polarization at the Fermi level at low temperatures [25, 56], the Heusler alloys remain attractive for technical applications like spin-injection devices [57], spin-filters [58], tunnel junctions [59], or GMR devices [60, 61] due to their relatively high Curie temperature compared to these compounds [10].

NiMnSb is the half-metallic semi-Heusler compound which attracted a lot of experimental interest. Its half-metallic character in single crystals has been well-established by infrared absorption [62] and spin-polarized positron-annihilation [63, 64] experiments. Also high quality films of NiMnSb have been grown [65–73] but contrary to single crystals they are not half-metallic [25, 74–77]; a maximum value of 58% for the spin-polarization of NiMnSb was obtained by Soulen *et al.* [25]. These polarization values are consistent with a small perpendicular magnetoresistance measured for NiMnSb in a spin-valve structure [78, 79], a superconducting tunnel junction [59] and a tunnel magnetoresistive junction [80]. The loss of half-metallicity in the NiMnSb thin films is due to the segregation of Sb and Mn atoms to the surface, which is far from being perfect [81–84].

NiMnSb has attracted also considerable attention among theoreticians and several first-principles calculations have confirmed its half-metallic character [85–90]. Larson *et al.* have shown that the C1$_b$ structure of NiMnSb is the most stable with respect to an interchange of the atoms [91]. Orgassa *et al.* showed that a few percent of disorder induce states within the gap but do not destroy the half-metallicity [92]. Surfaces and interfaces with semiconductors have been found not to be half-metallic [93–99] but Wijs and de Groot as well as Debernardi *et al.* proposed that at some interfaces it is possible to restore the half-metallic character of NiMnSb [100, 101]. Finally, Kübler calculated the Curie temperature of NiMnSb [102] which was in excellent agreement with the experimental value of 770 K [10]. Doping in similar semi-Heusler compounds can be employed to tune their magnetic properties [103, 104].

Full-Heusler compounds were the first to be synthesized [105–107]. In a pioneering paper Kübler *et al.* studied the mechanisms stabilizing the ferro- or the antiferromagnetism in these compounds [108]. Japanese research groups were the first to predict the existence of half-metallicity in the case of full-Heusler compounds using *ab-initio* electronic structure calculations: Ishida and collaborators studied the Co$_2$MnZ compounds , where Z stands for Si and Ge [109–111], and Fujii and collaborators studied the Fe$_2$MnZ compounds [112]. But Brown *et al.* [113] using polarized neutron diffraction measurements have shown that there is a finite very small spin-down density of states (DOS) at the Fermi level instead of an
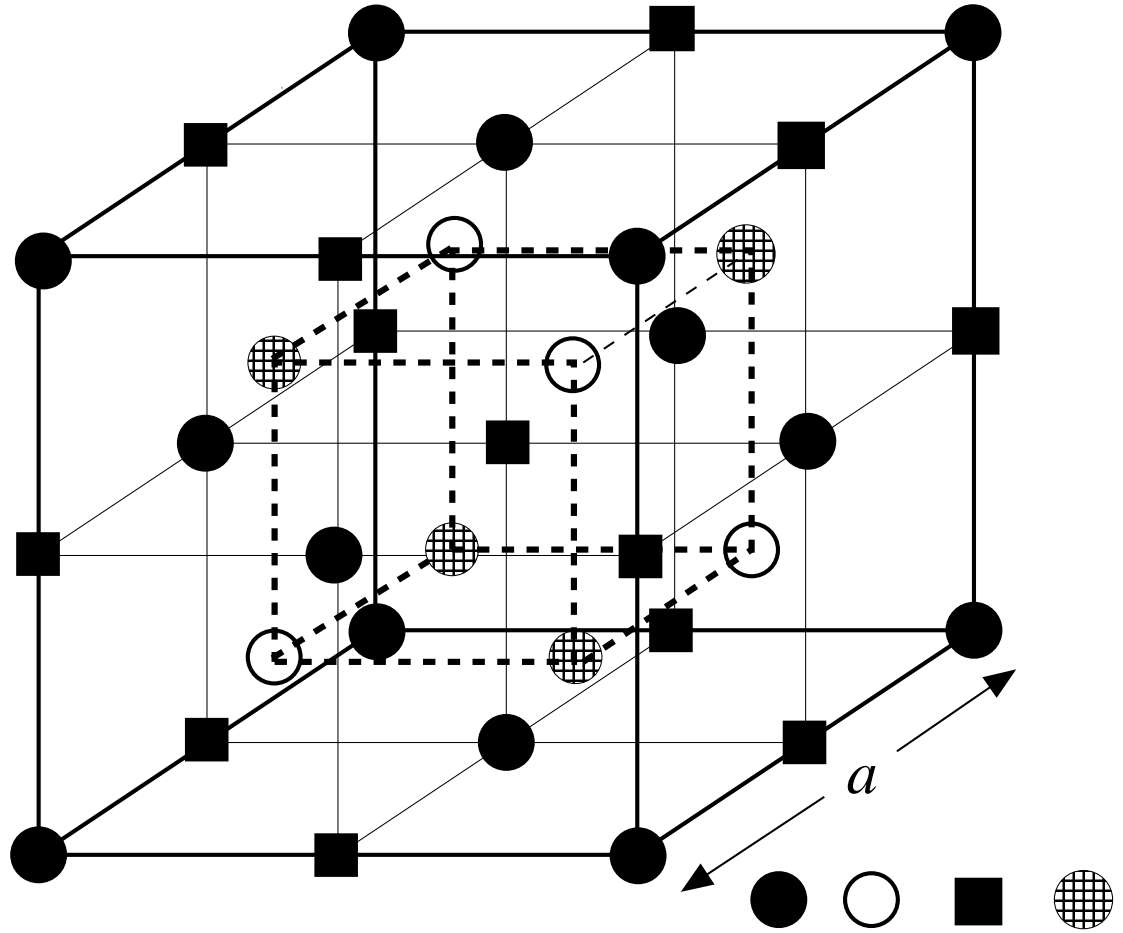
	A	B	C	D
Semi–Heuslers (C1$_b$) : XYZ	X	Y		Z
Full–Heuslers (L2$_1$) : X$_2$YZ	X	Y	X	Z
Quaternary Heuslers : (XX')YZ	X	Y	X'	Z
Inverse Heuslers (XA) : X$_2$YZ	X	X	Y	Z

FIG. 1. Schematic representation of the various structures of the semi- and full-Heusler compounds. In all cases the lattice is consisted of 4 interpenetrating f.c.c. lattices. Note also that if all atoms were identical, the lattice would be simply the b.c.c.

absolute gap in agreement with the *ab-initio* calculations of Kübler *et al.* for the Co$_2$MnAl and Co$_2$MnSn compounds [108]. Full-Heusler compounds became very popular for potential applications and several groups managed to grow Co$_2$MnGe and Co$_2$MnSi thin films [114–

122]. Geiersbach and collaborators have grown (110) thin films of Co_2MnSi, Co_2MnGe and Co_2MnSn using a metallic seed on top of a MgO(001) substrate [123, 124] and studied also the transport properties of multilayers of these compounds with normal metals [125]. But as Picozzi *et al.* and Galanakis *et al.* have shown the interfaces of such structures are not half-metallic [126–130]. Although, the cubic structure and ferromagnetism in these compounds is particular stable [131–133], it has been shown that defects and vacancies can lead to loss of the half-metallic character [134–138], although a small degree of disorder may lead to half-metallic ferrimagnetism instead of ferromagnetism [139, 140]. Finally, Kämmerer and collaborators managed to built magnetic tunnel junctions based on Co_2MnSi [141, 142]. Similar experiments have been undertaken by Inomata and collaborators using $Co_2Cr_{0.6}Fe_{0.4}Al$ as the magnetic electrode [143, 144].

In this review, we present a study of the basic electronic and magnetic properties of the half-metallic Heusler alloys. Analyzing the *ab-initio* results using the group-theory and simple models we explain the origin of the gap in both the semi- and full-Heusler alloys, which is fundamental for understanding their electronic and magnetic properties. For both families of compounds the total spin magnetic moment scales with the number of valence electron, thus opening the way to engineer new half-metallic Heusler alloys with the desired magnetic properties as the quaternary half-metallic ferromagnets, the so-called half-metallic antiferromagnets, the magnetic semiconductors including also the spin-gapless semiconductors.

II.   SEMI-HEUSLER COMPOUNDS

A.   Band Structure of Semi-Heusler Compounds

We will start our discussion from the semi-Heusler compounds and more precisely from NiMnSb which is the most studied representative of the half-metallic semi-Heuslers [19]. Figure 2 shows the density of states (DOS) of NiMnSb in a non-spin-polarized calculation and in a calculation correctly including the spin-polarization. Given are the local contributions to the density of states (LDOS) on the Ni-site, the Mn-site and the Sb-site. The calculations have been performed using the Vosko, Wilk and Nusair parametrization [145] for the local density approximation (LDA) to the exchange-correlation potential [146, 147] to solve the
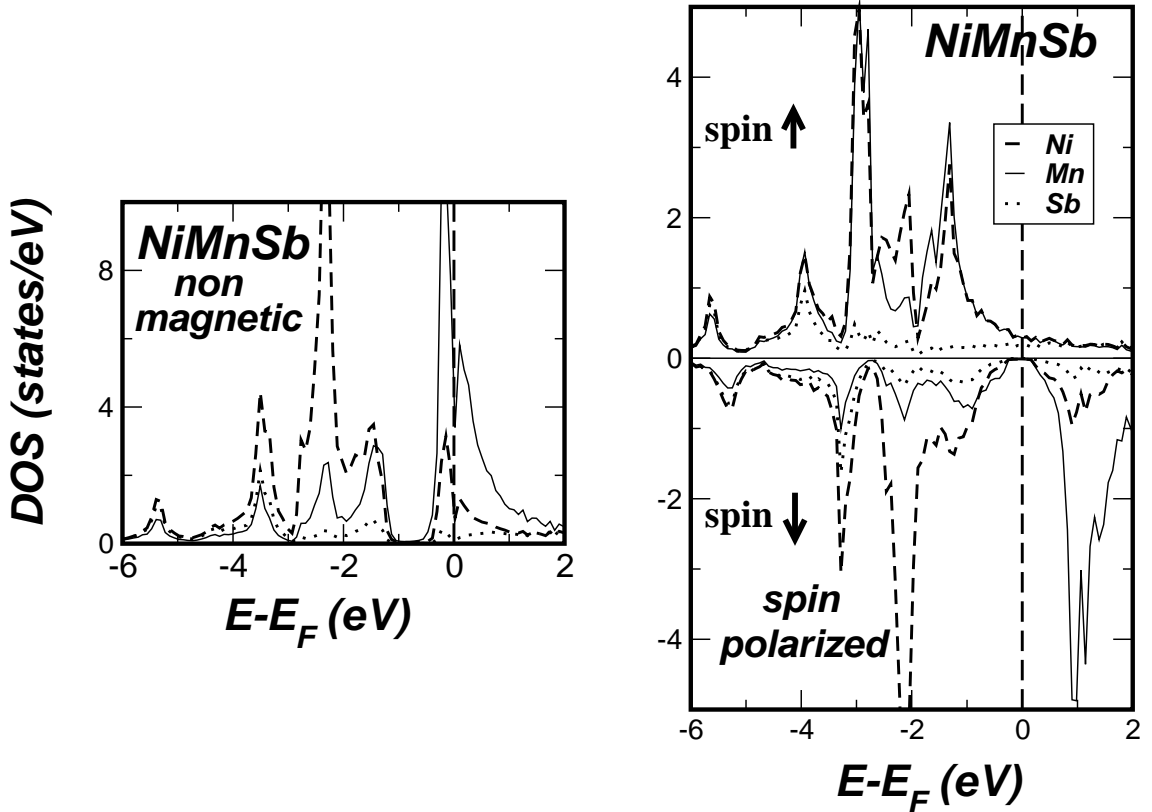
FIG. 2. Atom-resolved density of states (DOS) of NiMnSb for a non-magnetic (left) and ferromagnetic (right) calculation. The zero energy value corresponds to the Fermi level E_{F}.

Kohn-Sham equations within the full-potential screened Korringa-Kohn-Rostoker (FSKKR) method [148, 149].

In the non-magnetic case the DOS of NiMnSb has contributions from 4 different bands: Each Sb atom with the atomic configuration $5s^2 5p^3$ introduces a deep lying s band, which is located at about -12eV and is not shown in the figure, and three p-bands in the regions between -5.5 and -3eV. These bands are separated by a deep minimum in the DOS from 5 Ni d bands between -3 and -1eV, which themselves are separated by a sizeable band gap from the upper 5 d-bands of Mn. Since all atomic orbitals, i.e. the Ni d, the Mn d and the Sb sp orbitals hybridize with each other, all bands are hybrids between these states, being either of bonding or antibonding type. Thus the Ni d-bands contain a bonding Mn d admixture, while the higher Mn d-bands are antibonding hybrids with small Ni d-admixtures.

Equally the Sb p-bands exhibit strong Ni d- and somewhat smaller Mn d-contributions. This configuration for NiMnSb is energetically not stable. The Fermi energy lies in the middle of an antibonding band and the Mn atom can gain considerable exchange energy by forming a magnetic moment. Therefore the spin-polarized results show a considerably different picture. In the majority (spin ↑) band the Mn d states are shifted to lower energies and form a common d band with the Ni d states, while in the minority band (spin ↓) the Mn states are shifted to higher energies and are unoccupied, so that a band gap at E_F is formed separating the occupied d bonding from the unoccupied d-type antibonding states. Thus NiMnSb is a half-metal, with a band gap at E_F in the minority band and a metallic DOS at E_F in the majority band. The total magnetic moment, located mostly at the Mn atom, can be easily estimated to be exactly 4 μ_B. Note that NiMnSb has 22 valence electrons per unit cell, 10 from Ni, 7 from Mn and 5 from Sb. Since, due to the gap at E_F, in the minority band exactly 9 bands are fully occupied (1 Sb-like s band, 3 Sb-like p bands and 5 Ni-like d bands) and accommodate 9 electrons per unit cell, the majority band contains 22 - 9 = 13 electrons, resulting in a moment of 4 μ_B per unit cell. Notice that the compounds with 18 valence electrons like CoTiSb and FeVSn are well-known to be stable semiconductors [13–15].

As representative examples of the semi-Heuslers we will shortly discuss the electronic structure of the XMnSb compounds, with X being an element of the Co or Ni columns in the periodic table. These compounds are known experimentally to be ferromagnets with high Curie temperatures ranging between 500 K and 700 K for the Co, Ni, Pd and Pt compounds, while the Curie temperatures of the Ir and Rh compounds are around room temperature [10]. All six compounds (see figure 3) present a minority-spin band energy gap. As above Sb p states occupy the lowest part of the DOS shown in the figure, while the Sb s states are located ∼12 eV below the Fermi level. For all compounds under study the Fermi level is within the gap with the exception of PdMnSb and IrMnSb where it is close to the band edge. The DOS of all compounds is characterized by the large exchange-splitting of the Mn d states which is around 3 eV. This leads to large localized spin moments at the Mn site, the existence of which has been verified also experimentally [150, 151]. The localization of the spin magnetic moment stems from the fact that although the 3d valence electrons of Mn are itinerant, the spin-down electrons are almost excluded from the Mn site. In table I we present the calculated spin magnetic moments at the different sites for all the compounds
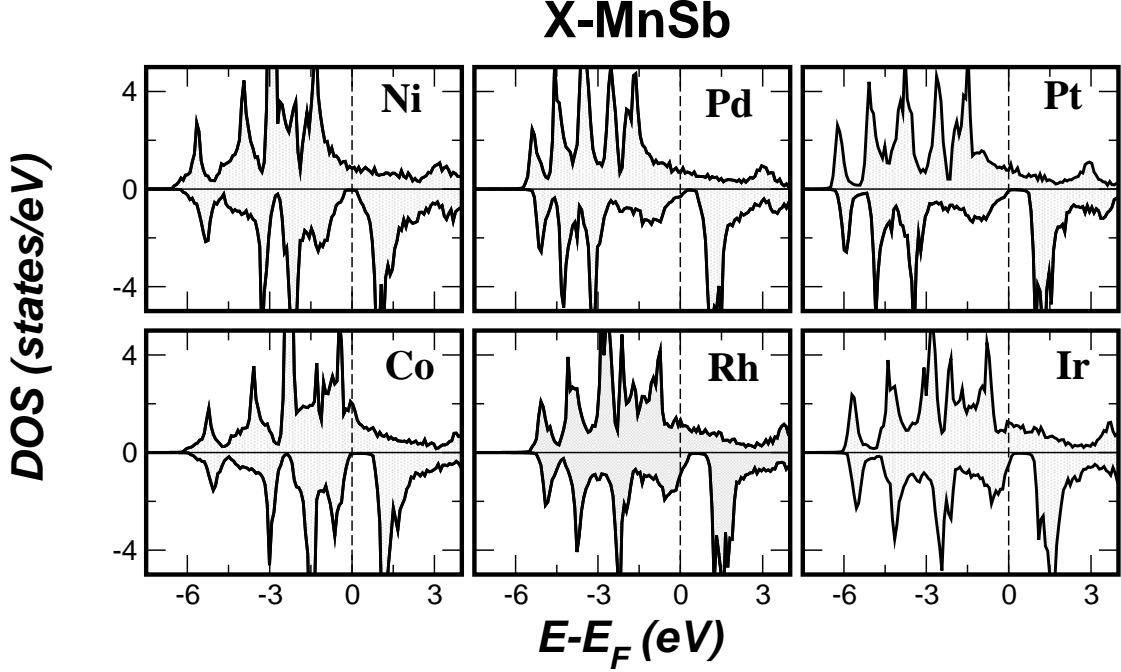
FIG. 3. DOS of XMnSb compounds for X= Ni, Pd, Pt and Co, Rh, Pd.

under study.

The total spin magnetic moment in μ_B is just the difference between the number of spin-up occupied states and the spin-down occupied states. As explained above, the number of occupied spin-down states is given by the number of spin down bands, i.e. 9, so that the number of occupied spin-up states is 22-9 = 13 for NiMnSb and the isovalent compounds with Pd and Pt, but 21-9 = 12 for CoMnSb, RhMnSb and IrMnSb and 20-9 = 11 for FeMnSb, provided that the Fermi level stays within the gap. Therefore one expects total moments of $4\mu_B$ for Ni-, Pd- and PtMnSb, 3 μ_B for the compounds with Co, Rh and Ir and 2 μ_B for FeMnSb. In general, for a total number Z_t of valence electrons in the unit cell, the total moment M_t is given by $M_t = Z_t - 18$, since with 9 electron states occupied in the minority band, $Z_t - 18$ is just the number of uncompensated electron spins. The local moment per unit cell as given in table I is close to 4 μ_B in the case of NiMnSb, PdMnSb and PtMnSb,

8

TABLE I. Calculated spin magnetic moments in μ_B for the XMnSb compounds using the FSKKR method. The total spin magnetic deviate from the ideal integer values due to the due to problems with the ℓ_{max} cutoff [260]. (The experimental lattice constants [10] have been used.)

$m^{spin}(\mu_B)$	X	Mn	Sb	Void	Total
NiMnSb	0.26	3.71	-0.06	0.05	3.96
PdMnSb	0.08	4.01	-0.11	0.04	4.02
PtMnSb	0.09	3.89	-0.08	0.04	3.94
CoMnSb	-0.13	3.18	-0.10	0.01	2.96
RhMnSb	-0.13	3.57	-0.14	0.00	3.29
IrMnSb	-0.19	3.33	-0.11	-0.00	3.02
FeMnSb	-0.70	2.72	-0.05	0.02	1.98

which is in agreement with the half-metallic character (or nearly half-metallic character in the case of PdMnSb) observed in figure 3. We also find that the local moment of Mn is not far away from the total number of 4 μ_B although there are significant (positive) contributions from the X-atoms and a negative contribution from the Sb atom. For the half-metallic CoMnSb and IrMnSb compounds the total moment is about 3 μ_B. Also the local moment of Mn is reduced, but only by about 0.5 μ_B. The reduction of the total moment to 3 μ_B is therefore accompanied by negative Co and Ir spin moments. The hybridization between Co and Mn is considerably larger than between Ni and Mn being a consequence of the smaller electronegativity difference and the larger extend of the Co orbitals. Therefore the minority valence band of CoMnSb has a larger Mn admixture than the one of NiMnSb whereas the minority conduction band of CoMnSb has a larger Co admixture than the Ni admixture in the NiMnSb conduction band, while the populations of the majority bands are barely changed. As a consequence, the Mn moment is reduced by the increasing hybridization , while the Co moment becomes negative. The table also shows that further substitution of Fe for Co leads also to a half-metallic alloy with a total spin magnetic moment of 2 μ_B as has been already shown by de Groot *et al.* in reference [152].

B. Origin of the Gap

The inspection of the local DOS shown in figure 2 for the ferromagnet NiMnSb shows that the DOS close to the gap is dominated by d-states: in the valence band by bonding hybrids with large Ni admixture and in the conduction band by the antibonding hybrids with large Mn admixture. Thus the gap originates from the strong hybridization between the d states of the higher valent and the lower valent transition metal atoms. This is shown schematically in figure 4. Therefore the origin of the gap is somewhat similar to the gap in compound semiconductors like GaAs which is enforced by the hybridization of the lower lying As sp-states with the energetically higher Ga sp-states. Note that in the C1$_b$-structure the Ni and Mn sublattices form a zinc-blende structure, which is important for the formation the gap. The difference with respect to GaAs is than only, that 5 d-orbitals, i.e. 3 t_{2g} and 2 e_g orbitals, are involved in the hybridization, instead of 4 sp^3-hybrids in the compound semiconductors.

The gap in the half-metallic $C1_b$ compounds is normally an indirect gap , with the maximum of the valence band at the Γ point and the minimum of the conduction band at the X-point. For NiMnSb we obtain a band gap of about 0.5 eV, which is in good agreement with the experiments of Kirillova and collaborators [62], who, analyzing their infrared spectra, estimated a gap width of ~ 0.4 eV. As seen already from figure 3 the gap of CoMnSb is considerable larger (~ 1 eV) and the Fermi level is located at the edge of the minority valence band.

As it is well-known, the local density approximation (LDA) and the generalized gradient approximation (GGA) strongly underestimate the values of the gaps in semiconductors, typically by a factor of two. However, very good values for these gaps are obtained in the so-called GW approximation of Hedin and Lundqvist [153], which describes potential in semiconductors very well. On the other hand the minority gap in the half-metallic systems might be better described by the LDA and GGA since in these system the screening is metallic.
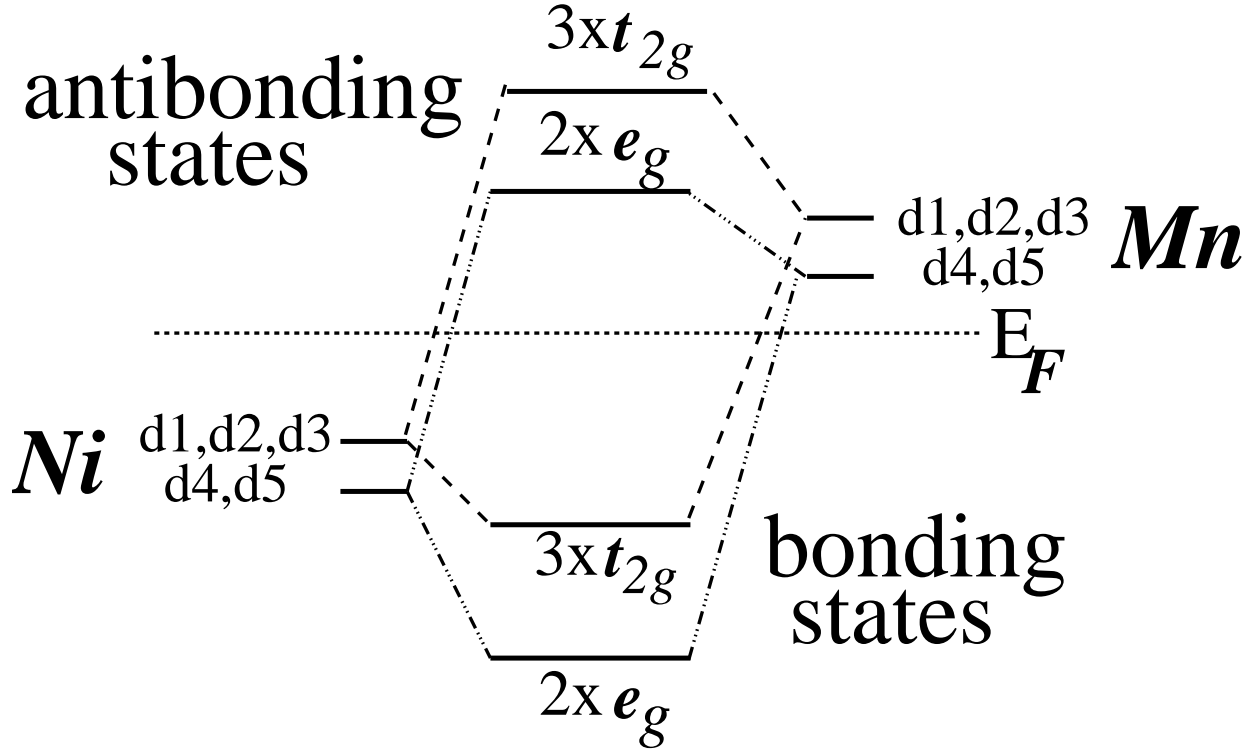
FIG. 4. Schematic illustration of the origin of the gap in the minority band in semi-Heusler alloys and in compound semiconductors: The energy levels of the energetically lower lying bonding hybrids are separated from the energy levels of the antibonding hybrids by a gap, such that only the bonding states are occupied. Due to legibility reasons, we use d1, d2 and d3 to denote the d_{xy}, d_{yx} and d_{zx} orbitals, respectively, and d4, d5 for the d_{r^2}, $d_{x^2-y^2}$ orbitals.

C. Role of sp-Elements

While the sp-elements are not responsible for the existence of the minority gap, they are nevertheless very important for the physical properties of the Heusler alloys and the structural stability of the $C1_b$ structure, as we discuss in the following.

While an Sb atom has 5 valence electrons ($5s^2$, $5p^3$), in the NiMnSb compound each Sb atom introduces a deep lying s-band, at about -12 eV, and three p-bands below the center of the d-bands. These bands accommodate a total of 8 electrons per unit cell, so that formally Sb acts as a triple charged Sb^{3-} ion. Analogously, a Te-atom behaves in these compounds as a Te^{2-} ion and a Sn-atom as a Sn^{4-} ion. This does not mean, that locally such a large charge transfer exists. In fact, the s- and p-states strongly hybridize with the transition-metal d-states and the charge in these bands is delocalized and locally Sb even looses about

11

one electron, if one counts the charge in the Wigner-Seitz cells. What counts is that the s- and p-bands accommodate 8 electrons per unit cell, thus effectively reducing the d-charge of the transition-metal atoms.

This is nicely illustrated by the existence of the semiconducting compounds CoTiSb and NiTiSn. Compared to CoTiSb, in NiTiSn the missing p-charge of the Sn atom is replaced by an increased d charge of the Ni atom, so that in both cases all 9 valence bands are occupied.

The sp-atom is very important for the structural stability of the Heusler alloys. For instance, it is difficult to imagine that the half-metallic NiMn and PtMn alloys with zinc-blende structure actually exist, since metallic alloys prefer highly coordinated structures like fcc, bcc, hcp etc. Therefore the sp-elements are decisive of the stability of the $C1_b$ compounds. A careful discussion of the bonding in these compounds has been recently published by Nanda and Dasgupta [154] using the crystal orbital Hamiltonian population (COHP) method. For the semiconductor FeVSb they find that while the largest contribution to the bonding arises from the V-d – Fe-d hybridization, contributions of similar size arise also from the Fe-d – Sb-p and the V-d – Sb-p hybridization. Similar results are also valid for the semiconductors like CoTiSb and NiTiSn and in particular for the half-metal NiMnSb. Since the majority d-band is completely filled, the major part of the bonding arises from the minority band, so that similar arguments as for the semiconductors apply.

Another property of the sp-elements is worthwhile to mention: substituting the Sb atom in NiMnSb by Sn, In or Te destroys the half-metallicity [20]. This is in contrast to the substitution of Ni by Co or Fe, which is documented in table I. The total moment of 4 μ_B for NiMnSb is reduced to 3 μ_B in CoMnSb and 2 μ_B in FeMnSb, thus preserving half-metallicity. In NiMnSn the total moment is reduced to 3.3 μ_B (instead of 3) and in NiMnTe the total moment increases only to 4.7 μ_B (instead of 5). Thus by changing the sp-element it is rather difficult to preserve the half-metallicity, since the density of states changes more like in a rigid band model [20].

D. Slater-Pauling Behavior

As discussed above the total moment of the half-metallic $C1_b$ Heusler alloys follows the simple rule: $M_t = Z_t - 18$, where Z_t is the total number of valence electrons. In short, the total number of electrons Z_t is given by the sum of the number of spin-up and spin-down

electrons, while the total moment M_t is given by the difference

$$Z_t = N_\uparrow + N_\downarrow \quad , \quad M_t = N_\uparrow - N_\downarrow \quad \rightarrow \quad M_t = Z_t - 2N_\downarrow \tag{1}$$

Since 9 minority bands are fully occupied, we obtain the simple "rule of 18" for half-metallicity in $C1_b$ Heusler alloys

$$M_t = Z_t - 18 \tag{2}$$

the importance of which has been recently pointed out by Jung et al. [155] and Galanakis et al. [20]. It is a direct analogue to the well-known Slater-Pauling behavior of the binary transition metal alloys [156–158]. The difference with respect to these alloys is, that in the semi-Heusler alloys the minority population is fixed to 9, so that the screening is achieved by filling the majority band, while in the transition metal alloys the majority band is filled with 5 d-states and charge neutrality is achieved by filling the minority states. Therefore in the transition-metal alloys the total spin magnetic moment is given by $M_t = 10 - Z_t$. Similar rules with integer total moments are also valid for other half-metals, e.g. for the full-Heusler alloys like Co_2MnGe with $L2_1$ structure. For these alloys we will in section 3 derive the "rule of 24": $M_t = Z_t - 24$, with arises from the fact that the minority band contains 12 electrons. For the half-metallic zinc-blende compounds like CrAs the rule is: $M_t = Z_t - 8$, since the minority As-like valence bands accommodate 4 electrons [28–30]. In all cases the moments are integer.

In figure 5 we have gathered the calculated total spin magnetic moments for the semi-Heusler alloys which we have plotted as a function of the total number of valence electrons. The dashed line represents the rule $M_t = Z_t - 18$ obeyed by these compounds. The total moment M_t is an integer quantity, assuming the values 0, 1, 2, 3, 4 and 5 if $Z_t \geq 18$. The value 0 corresponds to the semiconducting phase and the value 5 to the maximal moment when all 10 majority d-states are filled. Firstly we varied the valence of the lower-valent (*i.e.* magnetic) transition metal atom. Thus we substitute V, Cr and Fe for Mn in the NiMnSb and CoMnSb compounds using the experimental lattice constants of the two Mn compounds. For all these compounds we find that the total spin magnetic moment scales accurately with the total charge and that they all present the half-metallicity.

As a next test we have substituted Fe for Mn in CoMnSb and NiMnSb, but both CoFeSb and NiFeSb loose their half-metallic character. In the case of NiFeSb the majority d-states are already fully occupied as in NiMnSb, thus the additional electron has to be screened
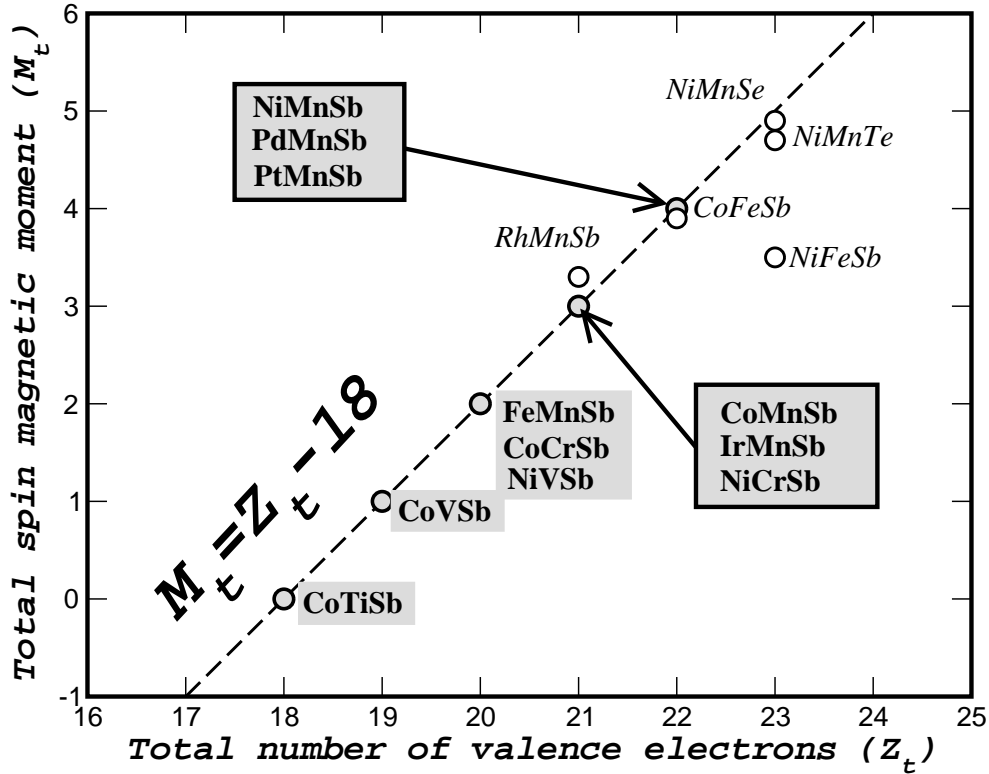
FIG. 5. Calculated total spin moments for all the studied semi Heusler alloys. The dashed line represents the Slater-Pauling behavior. With hollow circles we present the compounds deviating from the SP curve. Some experimental values for bulk systems near the SP curve from reference [10]: NiMnSb 3.85 μ_B, PdMnSb 3.95 μ_B, PtMnSb 4.14 μ_B and finally CoTiSb non-magnetic.

by the minority d-states, so that the Fermi level falls into the minority Fe states and the half-metallicity is lost; for half-metallicity a total moment of 5 μ_B would be required which is clearly not possible. For CoFeSb the situation is more delicate. This system has 22 valence electrons and if it would be a half-metal, it should have a total spin-moment of 4 μ_B as NiMnSb. In reality our calculations indicate that the Fermi level is slightly above the gap and the total spin-moment is slightly smaller than 4 μ_B. The Fe atom possesses a comparable spin-moment in both NiFeSb and CoFeSb compounds contrary to the behavior of the V, Cr and Mn atoms. Except NiFeSb other possible compounds with 23 valence electrons are NiMnTe and NiMnSe. We have calculated their magnetic properties using

the lattice constant of NiMnSb. As shown in figure 5, NiMnSe almost makes the 5 μ_B (its total spin moment is 4.86 μ_B) and is nearly half-metallic, while its isovalent, NiMnTe, has a slightly smaller spin moment. NiMnSe and NiMnTe show big changes in the majority band compared to systems with 22 valence electrons as NiMnSb or NiMnAs, since antibonding $p\text{-}d$ states, which are usually above E_F, are shifted below the Fermi level, thus increasing the total moment to nearly 5 μ_B.

III. FULL HEUSLER COMPOUNDS

A. Electronic Structure

The second family of Heusler alloys, which we discuss, are the full-Heusler alloys. We consider in particular compounds containing Co and Mn, as these are the full-Heusler alloys that have attracted most of the attention. They are all strong ferromagnets with high Curie temperatures (above 600 K) and except the Co_2MnAl they show very little disorder [10]. They adopt the $L2_1$ structure shown in figure 1. Each Mn or sp atom has eight Co atoms as first neighbors, sitting in an octahedral symmetry position, while each Co has four Mn and four sp atoms as first neighbors and thus the symmetry of the crystal is reduced to the tetrahedral one. The Co atoms occupying the two different sublattices are chemically equivalent as the environment of the one sublattice is the same as the environment of the second one but rotated by 90°. The occupancy of two fcc sublattices by Co (or in general by X) atoms distinguishes the full-Heusler alloys with the $L2_1$ structure from the semi-Heusler compounds with the $C1_b$ structure, like $e.g.$ CoMnSb, where only one sublattice is occupied by Co atoms and the other one is empty. Although in the $L2_1$ structure, the Co atoms are sitting on second neighbor positions, their interaction is important to explain the magnetic properties of these compounds as we will show in the next section. Finally, it should be noted that orbital magnetism in these compounds plays a minor role and thus can be neglected when discussing their magnetic properties [159]

In figure 6 we have gathered the spin-resolved density of states (DOS) for the Co_2MnAl, Co_2MnGa, Co_2MnSi and Co_2MnGe compounds calculated using the FSKKR. Firstly as shown by photoemission experiments by Brown et $al.$ in the case of Co_2MnSn [160] and verified by our calculations, the valence band extends around 6 eV below the Fermi level

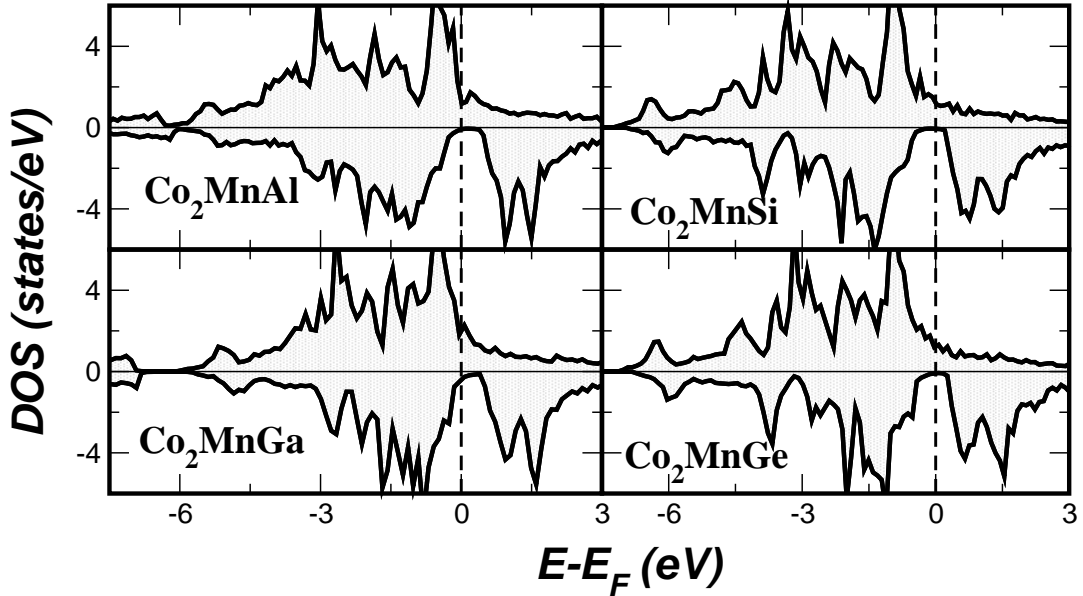FIG. 6. Total DOS for the Co$_2$MnZ compounds with Z= Al, Si, Ge, Sn compounds

and the spin-up DOS shows a large peak just below the Fermi level for these compounds. Although Ishida *et al.* [109, 110] predicted them to be half-metals with small spin-down gaps ranging from 0.1 to 0.3 eV depending on the material, our previous calculations showed a very small DOS at the Fermi level, in agreement with the ASW results of Kübler et al. [158] for Co$_2$MnAl and Co$_2$MnSn. However a recalculation of our KKR results with a higher ℓ-cut-off of $\ell_{\max} = 4$ restores the gap and we obtain good agreement with the results of Picozzi et al. using the FLAPW method. The gap is an indirect gap , with the maximum of the valence band at Γ and the minimum of the conduction band at the X-point. In the case of the full-Heusler alloys each Mn atom has eight Co atoms as first neighbors instead of four as in CoMnSb and the hybridization effect is very important decreasing even further the Mn spin moment to less than 3 μ_B except in the case of Co$_2$MnSn where it is comparable to the CoMnSb compound. The Co atoms are ferromagnetically coupled to the Mn spin moments

16

TABLE II. Calculated spin magnetic moments in μ_B using the experimental lattice constants (see reference [10]) for the Co_2MnZ compounds, where Z stands for the sp atom.

$m^{spin}(\mu_B)$	Co	Mn	Z	Total
Co_2MnAl	0.77	2.53	-0.10	3.97
Co_2MnGa	0.69	2.78	-0.09	4.06
Co_2MnSi	1.02	2.97	-0.07	4.94
Co_2MnGe	0.98	3.04	-0.06	4.94
Co_2MnSn	0.93	3.20	-0.08	4.98

and they posses a spin moment that varies from ~ 0.7 to $1.0\ \mu_B$. The Co moment is large and positive and arises basically from two unoccupied Co bands in the minority conduction band, as explained below. Therefore both Co atoms together can have a moment of about $2\ \mu_B$, if all majority Co states are occupied. This is basically the case for Co_2MnSi, Co_2MnGe and Co_2MnSn (see table II). In contrast to this the sp atom has a very small negative moment which is one order of magnitude smaller than the Co moment. The negative sign of the induced sp moment characterizes most of the studied full and semi Heusler alloys with very few exceptions. The compounds containing Al and Ga have 28 valence electrons and the ones containing Si, Ge and Sn 29 valence electrons. The first compounds have a total spin magnetic moment of $4\mu_B$ and the second ones of $5\ \mu_B$ which agree with the experimental deduced moments of these compounds [161, 162]. So it seems that the total spin magnetic moment , M_t, is related to the total number of valence electrons, Z_t, by the simple relation: $M_t = Z_t - 24$, while in the semi-Heusler alloys the total magnetic moment is given by the relation $M_t = Z_t - 18$. In the following section we will analyze the origin of this rule.

B. Origin of the gap in Full-Heusler Alloys

Since, similar to the semi-Heusler alloys, the four sp-bands are located far below the Fermi level and thus are not relevant for the gap, we consider only the hybridization of the 15 d states of the Mn atom and the two Co atoms. For simplicity we consider only the d-states at the Γ point, which show the full structural symmetry. We will give here a qualitative picture, since a thorough group theoretical analysis has been given in reference [21]. Note that the

Co atoms form a simple cubic lattice and that the Mn atoms (and the Ge atoms) occupy the body centered sites and have 8 Co atoms as nearest neighbors. Although the distance between the Co atoms is a second neighbors distance, the hybridization between these atoms is qualitatively very important. Therefore we start with the hybridization between these Co atoms which is qualitatively sketched in figure 7. The 5 d-orbitals are divided into the twofold degenerate d_{r^2}, $d_{x^2-y^2}$ and the threefold degenerate d_{xy}, d_{yx}, d_{zx} states. The e_g orbitals (t_{2g} orbitals) can only couple with the e_g orbitals (t_{2g} orbitals) of the other Co atom forming bonding hybrids , denoted by e_g (or t_{2g}) and antibonding orbitals , denoted by e_u (or t_{1u}). The coefficients in front of the orbitals give the degeneracy.

In a second step we consider the hybridization of these Co-Co orbitals with the Mn d-orbitals. As we show in the right-hand part of figure 7, the double degenerated e_g orbitals hybridize with the d_{r^2} and $d_{x^2-y^2}$ of the Mn that transform also with the same representation. They create a doubly degenerate bonding e_g state that is very low in energy and an antibonding one that is unoccupied and above the Fermi level. The $3 \times t_{2g}$ Co orbitals couple to the $d_{xy,yx,zx}$ of the Mn and create 6 new orbitals, 3 of which are bonding and are occupied and the other three are antibonding and high in energy. Finally the $2 \times e_u$ and $3 \times t_{1u}$ Co orbitals can not couple with any of the Mn d-orbitals since none of these is transforming with the u representations and they are orthogonal to the Co e_u and t_{1u} states. With respect to the Mn and the sp-atoms these states are therefore non-bonding. The t_{1u} states are below the Fermi level and they are occupied while the e_u are just above the Fermi level. Thus in total 8 minority d-bands are filled and 7 are empty.

Therefore all 5 Co-Mn bonding bands are occupied and all 5 Co-Mn antibonding bands are empty, and the Fermi level falls in between the 5 non-bonding Co bands, such that the three t_{1u} bands are occupied and the two e_u bands are empty. The maximal moment of the full Heusler alloys is therefore 7 μ_B per unit cell, which is achieved, if all majority d-states are occupied.

C. Slater-Pauling behavior of the Full-Heusler alloys

Following the above discussion we will investigate the Slater-Pauling behavior and in figure 8 we have plotted the total spin magnetic moments for all the compounds under study as a function of the total number of valence electrons. The dashed line represents
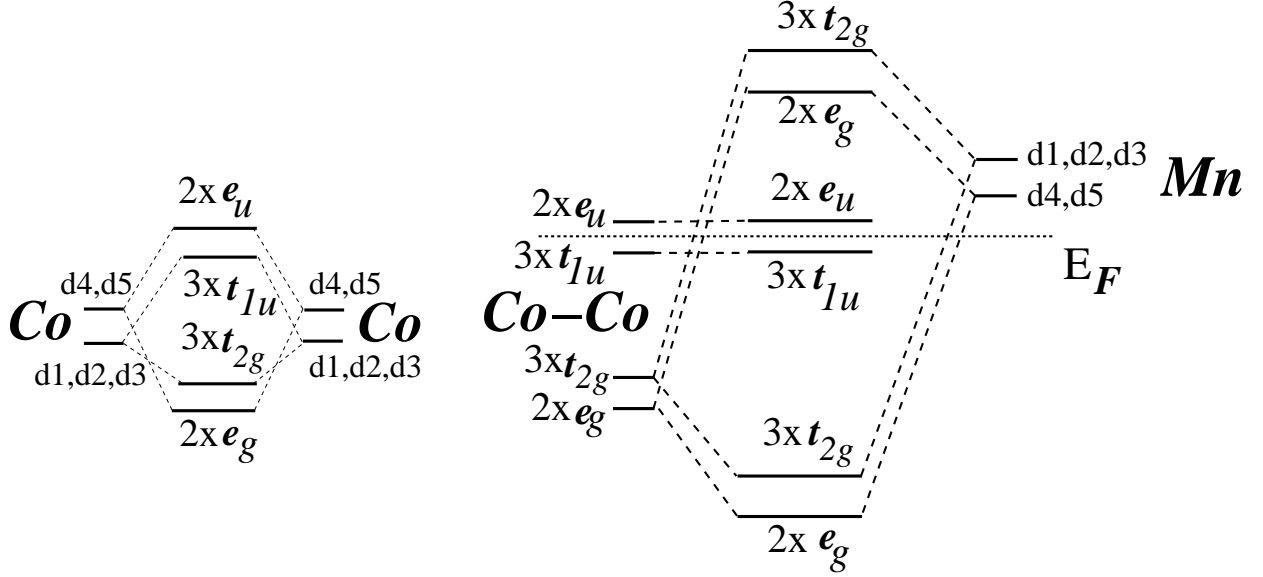
FIG. 7. Schematic illustration of the origin of the gap in the minority band in full-Heusler alloys. Due to legibility reasons, we use d1, d2 and d3 to denote the d_{xy}, d_{yx} and d_{zx} orbitals, respectively, and d4, d5 for the d_{r^2}, $d_{x^2-y^2}$ orbitals.

the half metallicity rule: $M_t = Z_t - 24$ of the full Heusler alloys. This rule arises from the fact that the minority band contains 12 electrons per unit cell: 4 are occupying the low lying s and p bands of the sp element and 8 the Co-like minority d bands ($2 \times e_g$, $3 \times t_{2g}$ and $3 \times t_{1u}$), as explained above (see figure 7). Since 7 minority bands are unoccupied, the largest possible moment is 7 μ_B and occurs when all majority d-states are occupied.

Overall we see that many of our results coincide with the Slater-Pauling curve. Some of the Rh compounds show small deviations which are more serious for the Co$_2$TiAl compound. We see that there is no compound with a total spin magnetic moment of 7 μ_B or even 6 μ_B. Moreover we found also examples of half-metallic materials with less than 24 electrons, Mn$_2$VGe with 23 valence electrons and Mn$_2$VAl with 22 valence electrons. Firstly, we have calculated the spin moments of the compounds Co$_2$YAl where Y= Ti, V, Cr, Mn and Fe. The compounds containing V, Cr and Mn show a similar behavior. As we substitute Cr for Mn, which has one valence electron less than Mn, we depopulate one Mn spin-up state and thus the spin moment of Cr is around 1 μ_B smaller than the Mn one while the Co moments are practically the same for both compounds. Substituting V for Cr has a larger effect since also the Co spin-up DOS changes slightly and the Co magnetic moment is increased by about 0.1 μ_B compared to the other two compounds and V possesses a small moment of 0.2

μ_B. This change in the behavior is due to the smaller hybridization between the Co atoms and the V ones as compared to the Cr and Mn atoms. Although all three Co$_2$VAl, Co$_2$CrAl and Co$_2$MnAl compounds are on the SP curve as can be seen in figure 8, this is not the case for the compounds containing Fe and Ti. If the substitution of Fe for Mn followed the same logic as the one of Cr for Mn then the Fe moment should be around 3.5 μ_B which is a very large moment for the Fe site. Therefore it is energetically more favorable for the system that also the Co moment is increased, as it was also the case for the other systems with 29 electrons like Co$_2$MnSi, but while the latter one makes it to 5 μ_B, Co$_2$FeAl reaches a value of 4.9 μ_B. In the case of Co$_2$TiAl, it is energetically more favorable to have a weak ferromagnet than an integer moment of 1 μ_B as it is very difficult to magnetize the Ti atom. Even in the case of the Co$_2$TiSn the calculated total spin magnetic moment of 1.78 μ_B (compared to the experimental value of 1.96 μ_B [163]) arises only from the Co atoms as was also shown experimentally by Pendl *et al.* [164], and the Ti atom is practically nonmagnetic and the latter compound fails to follow the SP curve.

As a second family of materials we have studied the compounds containing Fe. Fe$_2$VAl has in total 24 valence electrons and is a semi-metal , *i.e.* nonmagnetic with a very small DOS at the Fermi level, as it is already known experimentally [165–168]. All the studied Fe compounds follow the SP behavior as can be seen in figure 8. In the case of the Fe$_2$CrAl and Fe$_2$MnAl compounds the Cr and Mn atoms have spin moments comparable to the Co compounds and similar DOS. In order to follow the SP curve the Fe in Fe$_2$CrAl is practically nonmagnetic while in Fe$_2$MnAl it has a small negative moment. When we substitute Si for Al in Fe$_2$MnAl, the extra electron exclusively populates Fe spin-up states and the spin moment of each Fe atom is increased by 0.5 μ_B contrary to the corresponding Co compounds where also the Mn spin moment was considerably increased. Finally we calculated as a test Mn$_2$VAl and Mn$_2$VGe that have 22 and 23 valence electrons, respectively, to see if we can reproduce the SP behavior not only for compounds with more than 24, but also for compounds with less than 24 electrons. As we have already shown Fe$_2$VAl is nonmagnetic and Co$_2$VAl, which has two electrons more, has a spin moment of 2 μ_B. Mn$_2$VAl has two valence electrons less than Fe$_2$VAl and its total spin moment is $-2\,\mu_B$ and thus it follows the SP behavior [169]; negative total spin moment means that the "minority" band with the gap has more occupied states than the "majority" one.

As we have already mentioned the maximal moment of a full-Heusler alloy is seven μ_B,
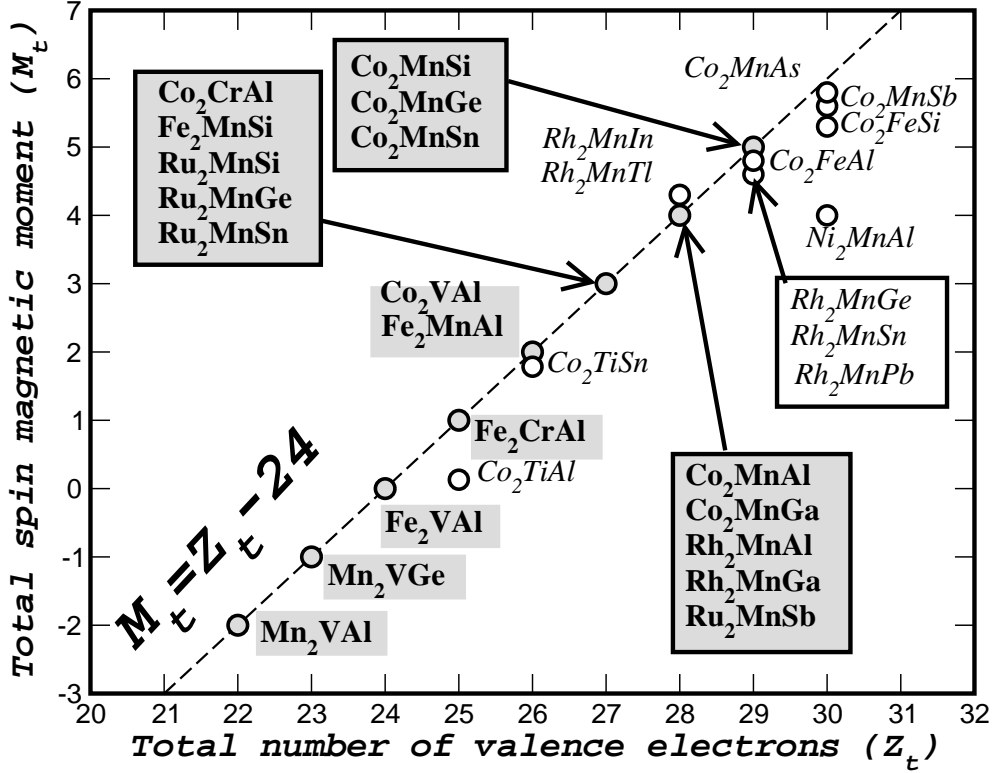
FIG. 8. Calculated total spin moments for all the studied full Heusler alloys. The dashed line represents the Slater-Pauling behavior. With open circles we present the compounds deviating from the SP curve. Some experimental values for bulk systems near the SP curve from reference [10]: Co$_2$MnAl 4.01 μ_B, Co$_2$MnSi 5.07 μ_B, Co$_2$MnGa 4.05 μ_B, Co$_2$MnGe 5.11 μ_B, Co$_2$MnSn 5.08 μ_B, Co$_2$FeSi 5.9 μ_B, Mn$_2$VAl -1.82 μ_B and finally Fe$_2$VAl non-magnetic.

and should occur, when all 15 majority d states are occupied. Analogously for a semi-Heusler alloy the maximal moment is 5 μ_B. However this limit is difficult to achieve, since due to the hybridization of the d states with empty sp-states of the transition metal atoms (sites X and Y in figure 1), d-intensity is transferred into states high above E_F, which are very difficult to occupy. Although in the case of semi-Heusler alloys, we could identify systems with a moment of nearly 5 μ_B, the hybridization is much stronger in the full-Heusler alloys so that a total moment of 7 μ_B seems to be impossible. Therefore we restrict our search to possible systems with 6 μ_B, i.e. systems with 30 valence electrons, but as shown also in
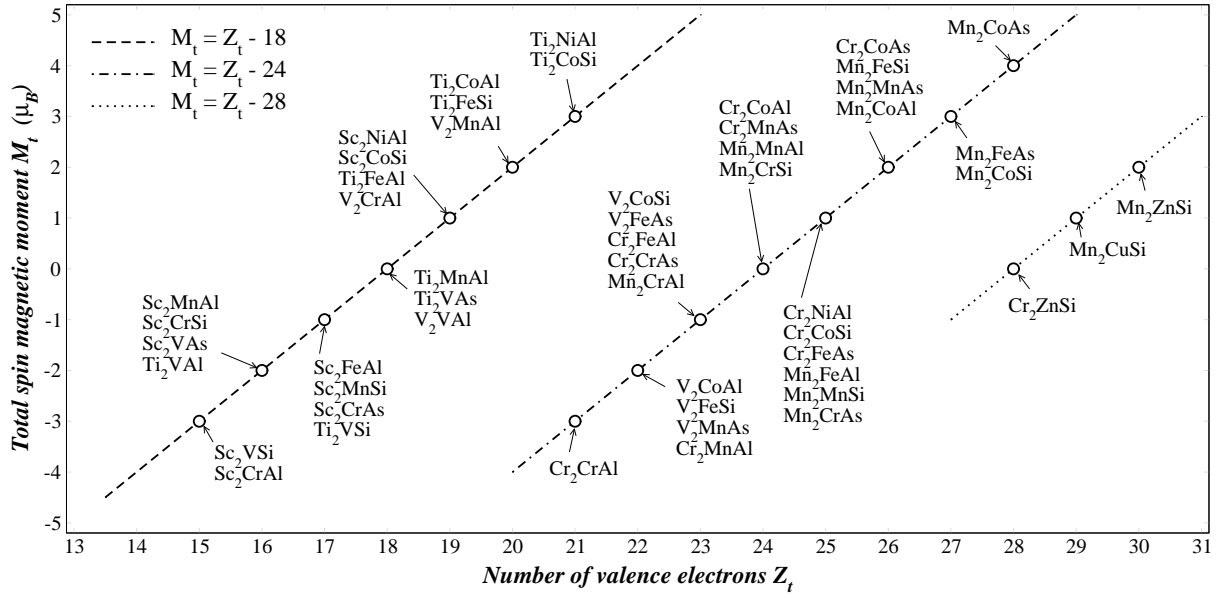
FIG. 9. Calculated total spin moments for several inverse Heusler compounds studied in reference [190]. The dashed lines represent the three variants of the Slater-Pauling behavior for these compounds.

figure 8, none of them makes exactly the 6 μ_B. Co_2MnAs shows the largest spin moment: 5.8 μ_B. The basic reason, why moments of 6 μ_B are so difficult to achieve, is that as a result of the strong hybridization with the two Co atoms the Mn atom cannot have a much larger moment than 3 μ_B. While due to the empty e_u-states the two Co atoms have no problem to contribute a total of 2 μ_B, the Mn moment is hybridization limited. Recent calculations employing the Hubbard U have shown that Co_2FeSi is susceptible of being a half-metal with a 6 μ_B total spin magnetic moment [170]. Further calculations by Tsirogiannis and Galanakis, using the on-site Coulomb parameters from reference [171], have shown that the result depends strongly on the choice of the functional accounting for the double term in these hybrid methods [172].

IV. INVERSE FULL-HEUSLER COMPOUNDS

Except the usual full-Heusler compounds studied in section III there exist also the so-called inverse full-Heusler compounds. The latter compounds have also the chemical formula X_2YZ but in their case the valence of the X transition-metal atom is smaller than the valence of the Y transition metal atom. As a consequence, the inverse Heusler compounds crystallize in the so-called XA or X_α structure, where the sequence of the atoms is X-X-Y-Z and the prototype is Hg_2TiCu [173]. Several inverse Heuslers have been studied using first-principles electronic structure calculations in literature [173–183]. In all cases the XA structure is energetically preferred to the $L2_1$ structure of the usual full-Heusler compounds where the sequence of the atoms is X-Y-X-Z. The latter has been also confirmed by experiments on Mn_2CoGa and Mn_2CoSn films as well as Co doped Mn_3Ga samples [184–187], but experiments on Mn_2NiSb revealed that the actual arrangement of the atoms at the various sites can be influenced by the preparing method [188]. Inverse Heuslers are interesting for applications since they combine coherent growth on semiconductors with large Curie temperatures which can exceed the 1000 K as in the case of Cr_2CoGa [189].

In reference [190], extensive first-principles calculations have been presented on the inverse full-Heusler compounds having the chemical formula X_2YZ where (X = Sc, Ti, V, Cr or Mn), (Z = Al, Si or As) and the Y ranged from Ti to Zn. Several of these compounds have been identified to be half-metallic magnets. The appearance of half-metallicity is associated in all cases to a Slater-Pauling behavior of the total spin-magnetic moment. It was shown that when X is Sc or Ti, the total spin magnetic moment per formula unit (or unit cell) in μ_B follows the rule $M_t = Z_t - 18$ where Z_t is the total number of valence electrons in the unit cell. When X = Cr- or Mn, the variant followed by M_t is $M_t = Z_t - 24$, and when X = V the form of the slater-Pauling rule was found to be material specific. The occurrence of these rules can be explained using simple hybridization arguments of the transition metal d-orbitals. In fact, when X is Cr or Mn the situation is similar to the usual Heusler compounds discussed above, but when X is Sc or Ti, the Fermi level in the minority-spin band structure is located below the non-bonding t_{1u} states discussed in section III leading to the other variant of the Slater-Pauling rule. In figure 9 we present for several inverse Heusler compounds the calculated total spin-magnetic moment in μ_B per formula unit as a function of the total number of valence electrons. Finally, a third variant of the Slater-Pauling rule occurs, as

TABLE III. Calculated equilibrium lattice constant and spin magnetic moments in μ_B for the LiMgPdSn-type Heusler compounds, where X is Co, obeying the $M_t = Z_t - 24$ Slater-Pauling rule using the FPLO method code [261, 262]. The total spin magnetic moment is given per formula unit (which coincides with the per unit cell value).

(XX')YZ	a(Å)	m^X	$m^{X'}$	m^Y	m^{total}	Z_t
(CoCr)TiAl	5.95	-0.23	-2.15	0.28	-2.00	22
(CoV)TiSi	5.90	-0.26	-1.67	-0.12	-2.00	22
(CoCr)VAl	5.82	-0.34	-1.28	0.59	-1.00	23
(CoMn)TiAl	5.86	-0.23	-1.03	0.23	-0.98	23
(CoCr)TiSi	5.80	-0.21	-0.92	0.09	-1.00	23
(CoV)TiAs	5.97	-0.13	-0.90	-0.03	-1.00	23
(CoMn)CrAl	5.71	0.66	-1.09	1.50	1.00	25
(CoFe)VAl	5.73	0.61	0.51	-0.09	0.97	25
(CoMn)VSi	5.65	0.67	-0.05	0.38	0.97	25
(CoFe)TiSi	5.73	0.58	0.65	-0.19	1.00	25
(CoCr)VAs	5.80	0.72	-0.41	0.68	1.00	25
(CoMn)TiAs	5.83	0.62	0.54	-0.15	1.00	25
(CoMn)VAs	5.77	1.15	0.47	0.35	2.00	26
(CoFe)MnAl	5.68	0.73	-0.18	2.59	3.00	27
(CoFe)CrSi	5.61	1.00	0.33	1.79	3.00	27
(CoMn)CrAs	5.75	1.06	-0.44	2.38	3.00	27
(CoFe)VAs	5.78	1.05	1.19	0.75	3.00	27
(CoFe)MnSi	5.60	0.79	0.55	2.81	4.00	28
(CoFe)CrAs	5.75	0.91	0.80	2.34	4.00	28
(CoFe)MnAs	5.74	0.94	0.99	3.12	5.00	29

shown in [190], when X is Cr or Mn and Y is Cu or Zn. In this case Cu or Zn d-states are completely occupied being in energy below the X d-states, and the half-metallic compounds follow a $M_t = Z_t - 28$ rule.

V.   LiMgPdSn-TYPE HEUSLER COMPOUNDS

Except the usual and inverse full-Heusler compounds, another full-Heuslers family is the LiMgPdSn-type ones; also known as LiMgPdSb-type Heusler compounds [191]. These are quaternary compounds with the chemical formula (XX')YZ where X, X' and Y are transition metal atoms. The valence of X' is lower than the valence of X atoms, and the valence of the Y element is lower than the valence of both X and X'. The sequence of the atoms along the fcc cube's diagonal is X-Y-X'-Z which is energetically the most stable [192]. A few LiMgPdSn-type half-metallic compounds have been studied [191, 193, 194]. Recent studied have been devoted to the study of a large series of such compounds.[195, 196]

More precisely in reference [196], first-principles electronic structure calculations have been employed to study the electronic and magnetic properties of the 60 LiMgPdSn-type multifunctional quaternary Heusler compounds. It was shown that most of the compounds were half-metals obeying the same Slater-Pauling rule for full-Heusler compounds, $M_t = Z_t - 24$, with only few exceptions. The driving force behind the Slater-Paling rule was shown to be the same hybridization scheme as in full-Heusler compounds. In table III, the calculated total and atom-resolved spin magnetic moments, for the case where X is Co, from reference [196] are presented.

VI.   DISORDERED QUATERNARY HEUSLER ALLOYS

We proceed our study by examining the behavior of the so-called quaternary Heusler alloys [22, 197–199]. In the latter compounds, one of the four sites is occupied by two different kinds of neighboring elements like $Co_2[Cr_{1-x}Mn_x]Al$ where the Y site is occupied by Cr or Mn atoms There is even the possibility of growing quinternary Heusler compounds where also the D site is occupied by two species of sp-atoms [200]. To perform this study we used the KKR method within the coherent potential approximation (CPA) as implemented by H. Akai [54], which has been already used with success to study the magnetic semiconductors [54]. For all calculations we assumed that the lattice constant varies linearly with the concentration x which has been verified for several quaternary alloys [10, 11]. To our knowledge from the systems under study only $Co_2Cr_{0.6}Fe_{0.4}Al$ has been studied experimentally [201–205].

We calculated the total spin moment for several quaternary alloys taking into account

several possible combinations of chemical elements and assuming in all cases a concentration increment of 0.1. The first possible case is when we have two different low-valent transition metal atoms at the Y site like $Co_2[Cr_{1-x}Mn_x]Al$. The total spin moment varies linearly between the 3 μ_B of Co_2CrAl and the 4 μ_B of Co_2MnAl. In the case of the $Co_2[Cr_{1-x}Fe_x]Al$ and $Co_2[Mn_{1-x}Fe_x]Al$ compounds and up to around $x=0.6$ the total spin moment shows the SP behavior but for larger concentrations it slightly deviates to account for the non-integer moment value of Co_2FeAl. The second case is when one mixes the *sp* elements, but as we just mentioned these compounds also obey the rule for the total spin moments. The third and final case is to mix the higher valent transition metal atoms like in $[Fe_{1-x}Co_x]_2MnAl$ and $[Rh_{1-x}Co_x]_2MnAl$ alloys. In the first case the total spin moment varies linearly between the 2 and 4 μ_B of Fe_2MnAl and Co_2MnAl compounds, respectively. Rh is isoelectronic to Co and for the second family of compounds we find a constant integer value of 4 μ_B for all the concentrations. A special case is Mn_2VAl which has less than 24 electrons and the total spin moment is -2 μ_B. If now we mix Mn and Co, we get a family of compounds where the total spin moment varies linearly between the -2 μ_B and the 2 μ_B and for $x=0.5$ we get the case of a paramagnetic compound consisting of magnetic elements. Thus all the compounds obey the rule $M_t=Z_t-24$, showing the Slater-Pauling behavior regardless of the origin of the extra charge.

As a rule of thumb we expect, that for two half-metallic alloys like XYZ and $X'YZ$ (or $XY'Z, XYZ'$), which both lay on the Slater-Pauling curve, also the mixtures like $X_{1-x}X'_xYZ$ lay on the Slater Pauling curve, with an average moment of $< M_t >= (1-x)M_t^{XYZ} + xM_t^{X'YZ}$. However, if these intermediate structures are stable, is not guaranteed in particular if the parent compounds are not neighbors on the Slater-Pauling curve..

VII. HALF-METALLIC ANTIFERROMAGNETS

A special case for applications are the compounds made up from magnetic elements with exactly 18 (in the case of semi-Heuslers) or 24, in the case of full-Heuslers, valence electrons which should have a total zero spin magnetic moment in case of half-metallicity. These alloys should be of special interest for applications since they create no external stray fields and thus exhibit minimal energy losses [206]. In literature they are named either half-metallic fully-compensated ferrimagnets (HM-FCF) [207] or half-metallic antiferromagnets

(HMAs) which was the initial term used by van Leuken and de Groot when studying the semi-Heusler compound CrMnSb in 1995 [208]. The HMA character of CrMnSb has been also confirmed by calculations made by Shaughnessy and collaborators [209]. Contrary to conventional antiferromagnets here the compensation of the spin magnetic moments stems from different magnetic sublattices, $e.g$ in CrMnSb Cr and Mn atoms have antiparallel spin magnetic moments of about the same magnitude [208]. However, in contrast to zero temperature limit in which the total magnetization vanishes, at finite temperatures spin fluctuations induce a net magnetization in HMAs leading to a ferrimagnetic state [210]. Except the semi-Heusler CrMnSb, also full-Heusler alloys with 24 valence electrons have been predicted to be HMAs including the Mn_3Ga [207, 211, 212], Cr_2MnZ (Z=P,As,Sb,Bi) alloys [173, 213, 214], the Co-doped Mn_2VZ (Z=Al,Si) half-metallic ferrimagnetic alloys [215] and the Cr-doped Co_2CrAl [216]. Heusler compounds are not the only family of alloys where the half-metallic anitferromagnetism has been predicted. Potential HMA candidates include also the double-perovskites [217–221], superlattice structures [222, 223], diluted magnetic semicondutors [224, 225] and even Fe-based superconductors [226].

A special case of interest would be full-Heusler compounds where X and Y are of the same chemical species. This may lead to an easier growth of these materials and thus to enhanced properties of devices based on them. Moreover in this case we would also avoid the degradation of the magnetic properties caused by impurities and atomic swaps when the X and Y are of different chemical species like in Co_2MnSi [227]. The cubic structure which results when X and Y are the same in full-Heusler is known as the $D0_3$ structure. We mentioned in the above paragraph that Mn_3Ga which has 24 valence electrons has been predicted to be a half-metallic antiferromagnet [207]. Several experiments have been lately devoted to the growth of high quality samples of Mn_3Ga alloy [212, 228, 229]. In Reference [177], Li et al have shown that also Mn_3Al which has 24 valence electrons is a HF-FCF and when Cr was substituted for Mn, Cr_3Al was found to have a total spin-magnetic moment of -3 μ_B in accordance to the Slater-Pauling rule for half-metallic Heusler compounds. Doping of Mn_3Al with vanadium leads to the loss of half-metallicity [230]. In a recent publication (reference [189]) it was shown that Cr_3Se which has also 24 valence electrons is almost a half-metal with an almost zero total spin magnetic moment. The Cr atoms in the unit cell were antiferromagnetically coupled giving rise to ferrimagnetic behavior and the estimated Curie temperature was as high as $\sim$ 700 K. Thus this compound is

attractive for spintronics applications. Moreover the entire $Cr_{2+x}Se$ family, with $0 \leq x \leq 1$, shows the half-metallic antiferromagnetic behavior [231]. We should mention finally that one could envisage of growing a half-metallic antiferromagnet by combing alternate layers of half-metallic ferromagnetic and ferrimagnetic Heusler compounds as suggested in reference [232].

VIII.   MAGNETIC SEMICONDUCTORS

Magnetic semiconductors are compounds combining both the semiconducting behavior with the magnetic properties. Such compounds can offer novel functionalities to spintronic and magnetoelectronic devices, *e.g.* they can act as spin-filter materials. Such materials can find application in magnetic tunnel junctions (MTJ). In usual MTJs the magnetic electrodes are separated by an insulating barrier and ballistic transport is achieved through the tunnelling of the electrons via the barrier. The alternative is to use a spin-filter materials as the barrier and have metallic electrodes. Then the probability for electrons tunnelling through the spin-filter barrier is different for the two spin-directions and the flow of a spin-polarized current can be achieved [233, 234]. Among Heusler compounds there are two families of compounds studied recently which are magnetic semiconductors and can be used as spin-filter materials: (i) (CoV)XAl with X being Ti, Zr or Hf which are ferromagnetic semiconductors [235], and (ii) (CrV)XAl with X being Ti, Zr or Hf which are fully-compensated ferrimagnetic semiconductors [236]. The latter also combine magnetic semiconducting behavior with zero magnetization leading to minimum energy losses in devices. In figure 10 we present the total density of states for (CoV)TiAl and (CrV)TiAl where the energy gaps in both spin-directions are present.

A special class are the so-called spin-gapless semiconductors. These materials combine the properties of half-metals and magnetic semiconductors, and they are actually magnetic semiconductors where there is an almost vanishing zero-width energy gap at the Fermi level in the majority-spin direction and a usual energy gap in the other spin-direction [237]. Spin-gapless semiconductors offer also novel functionalists due to their unique properties :(i) the mobility of carriers is considerably larger than in usual semiconductors, (ii) excited carriers include both electrons and holes which can be 100% spin-polarized simultaneously, and (iii) a vanishing amount of energy is enough to excite majority-spin electrons from the valence
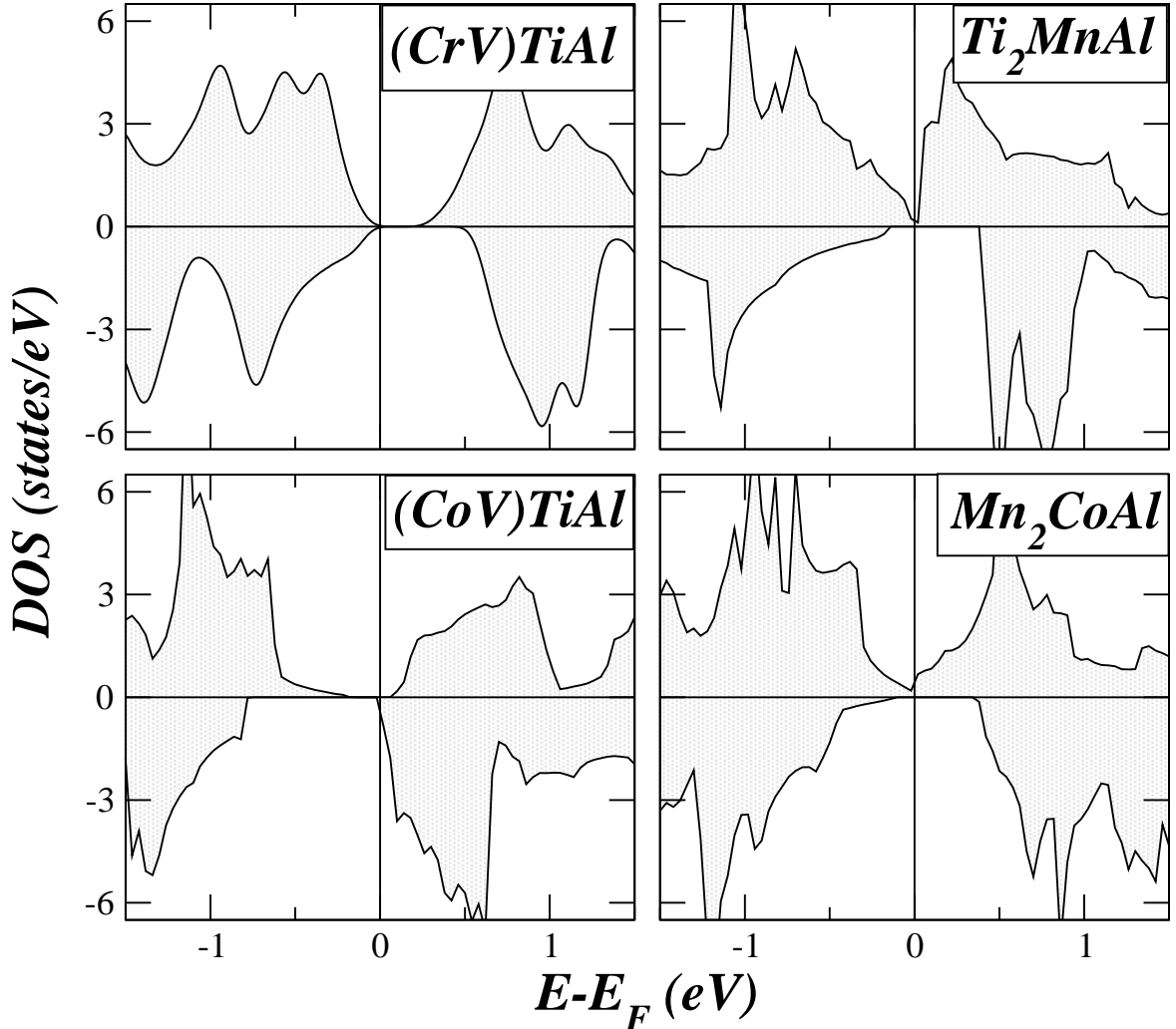
FIG. 10. Total DOS per formula unit around the Fermi level for four magnetic semiconductors. (CrV)TiAl is a fully-compensated ferrimagnetic semiconductor, (CoV)TiAl is a ferromagnetic semi-conductor, and Ti_2MnAl and Mn_2CoAl show a spin-gapless semiconducting behavior.

to the conduction band.

Although gapless-semiconductors are well known in literature [237], it was not until 2008, that Wang proposed that the doping of $PbPdO_2$, a gapless semiconductor, with transition metal atoms would lead to a spin gapless semiconductor [238, 239]. Experimental confirmation was offered in 2014 by Kim and collaborators who studied pollycrystalline films of Mn

and Co doped $PbPdO_2$ [240]. Among Heusler compounds several have been identified to be spin-gapless semiconductors [196, 241–243]. The main attention was given to Mn_2CoAl, an inverse full-Heusler compound, due to its successful growth in the form of films. In 2008 Liu and collaborators synthesized Mn_2CoAl using an arc-melting technique and found that it adopted the lattice structure of inverse full-Heuslers with a lattice constant of 5.8388 Å and a total spin magnetic moment of 1.95 μ_B per formula unit [174]. Electronic structure calculations yielded a ferrimagnetic state with a total spin magnetic moment of 1.95 μ_B per formula unit and an antiparallel coupling between the Mn nearest-neighboring atoms [174]. In 2011 Meinert and collaborators studied again theoretically this compound reproducing the calculated results of Liu *et al.* and also studied the exchange constants revealing that magnetic interactions in these compounds are short range direct interactions [244]. The breakthrough took place in 2013, when Ouardi et al identified the spin-gapless behavior of Mn_2CoAl and have confirmed it experimentally in bulk-like pollycrystalline films [245]. They found an experimental lattice constant of 5.798 Å, a Curie temperature of 720 K and a total spin magnetic per formula unit of 2 μ_B at a temperature of 5 K [245]. Following this research work, Jamer and collaborators have grown thin films of 70nm thickness on top of GaAs [246], but these films were found to deviate from the spin-gapless semiconducting behavior [247]. On the contrary films, grown on top of a thermally oxidized Si substrate, were found to be spin-gapless semiconductors with a Curie temperature of 550 K [248]. Ab-initio calculations of Skaftouros et al. identified among the inverse Heusler compounds another four potential SGS materials: Ti_2CoSi, Ti_2MnAl, Ti_2VAs and Cr_2ZnSi, with the latter three being also fully-compensated ferrimagnets, and V_3Al for which one V sublattice is not magnetic and the other two form a conventional antiferromagnet [241]. In figure 10 we present the total density of states for Mn_2CoAl and Ti_2MnAl presented in reference [241]. The spin-gapless semiconducting character of Ti_2MnAl was also confirmed by Jia *et al.* [249]. Wollman *et al.* [250] confirmed the conclusion of Meinert *et al.* that direct exchange interactions are responsible for the magnetic order in Mn_2CoAl studying a wide range of Mn_2-based Heusler compounds and predicted a Curie temperature of 740 K using the spherical approximation [251]. Skaftouros *et al.* discussed in detail the behavior of the total magnetic moment in inverse Heusler compounds including the spin-gapless materials [190]. Galanakis and collaborators have shown that defects keep the half-metallic character of Mn_2CoAl but destroy the spin-gapless semiconducting character [252]. Finally, recent

studies on the effect of doping of Mn_2CoAl with Co, Cu, V and Ti [253], as well as the anomalous Hall effect have appeared in literature [254].

IX. SPECIAL TOPICS

A. Exchange constants and Curie temperature

In reference [131] the exchange interactions are studied. In the case of semi-Heuslers, like NiMnSb and CoMnSb, the dominant interaction is the indirect interaction between the Mn atoms. Magnetic interactions are much more complex in the case of full- Heusler compounds, like Co_2MnSi and Co_2CrAl. Now there are three magnetic atoms in the unit cell and the ferromagnetic order is stabilized by the intersublattice interactions between the Mn(Cr) and Co atoms and between Co atoms belonging to different sublattices (see figure 1 for the structure) [131]. Contrary to the usual full-Heusler compounds, where both direct and indirect exchange interactions are present, the properties in the inverse Heusler compounds are dominated by short range interactions [175, 250]

To calculate the Curie temperature in magnetic materials usually either the mean-field (MFA) or the random-phase approximations (RPA) are employed. It has been shown in the case of Heusler compounds that RPA is more adequate to estimate the Curie temperature yielding values close to the experimental results [131]. The reason is that MFA is the numerical average over the magnons (spin-waves) while RPA is the harmonic average and thus in the latter the magnons with lower energy have a more significant impact on the Curie temperature which represents more accurately the experimental situation. In general Heusler compounds containing Mn atoms have Curie temperature much higher than the room temperature [10].

A cases of interest is the behavior of exchange constants upon doping. In reference [132], it was shown that in the case of the semi-Heusler compounds, NiMnSb and CoMnSb, the artificial shift of the Fermi level using a rigid band model results in a change in the relative strength of the Ruderman- Kittel-Kasuya-Yosida (RKKY)-like ferromagnetic and the superexchange antiferromagnetic interactions. The Curie temperature takes its maximum value when the Fermi level is located exactly at the middle of the minority-spin energy gap. This shift of the Fermi level in real systems can be achieved either by substituting Cu for

31

Ni or Co in NiMnSb/CoMnSb or by substituting Sb for Sn in AuMnSn. In both cases for large concentrations of Cu or Sb atoms the superexchange antiferromagnetic interaction dominates over the RKKY-like ferromagnetic interaction and antiferromagnetism becomes the stable magnetic state [103, 104].

B. Defects and vacancies

Spin-orbit interaction is mixing the two spin-channels and thus no real half-metal can exist. In reality, in Heusler compounds the effect of the spin-orbit coupling on the minority-spin band gap can be neglected [255]. Even when heavy elements are present like Sb in NiMnSb, the p-states of Sb are located low in energy and have vanishing weight near the Fermi level. Thus in bulk Heusler compounds only defects can affect their half-metallic character.

There are several derivatives of the initial ideal Heusler structures presented in figure 1 due either to atomic swaps or disorder [133]. In the structures derived from the occurrence of Co antisites in Co_2MnAl and Co_2MnSi compounds the half-metallicity is destroyed, while the Mn-Al(Si) swaps preserve the half-metallic character of the parent compounds [133]. In both Co_2MnAl and Co_2MnSi compounds when Fe or Cr is substituted for Mn the half-metallicity is preserved [134, 135]. In the case of Co_2MnSi, when a surplus of Mn or Si atoms is present, like in the $Co_2Mn_{1+x}Si_{1-x}$ compounds (with x ranging between -0.2 and 0.2), the half-metallicity is preserved contrary to the $Co_2Mn_{1+x}Al_{1-x}$ compounds where the half-metallicity is destroyed [134, 135]. A very interesting case of defects occurs when Cr or Mn atoms substitute Co atoms in Co_2CrZ or Co_2MnZ compounds with Z being a sp elements. The Cr and Mn impurity atoms are antiferromagnetically coupled to the Co atoms as well as to the Cr and Mn atoms sitting at the perfect C sites, and thus a half-metallic ferrimagnetic state occurs [139, 140].

Vacancies are also a very common defect occurring during the growth of samples of Heusler compounds. In the case of Co_2CrZ or Co_2MnZ compounds when the vacancy occurs at sites occupied by Co atoms the half-metallicity is destroyed contrary to vacancies at the Cr(Mn) or Z sites which leave the half-metallic character of the parent compounds unaltered [136]. In reference [138] it was shown for several families of Heusler compounds that the occurrence of vacancies at the A or C sites (see figure 1) occupied by the higher-valent

transition-metal atoms alters the local environment of the atoms destroying the half-metallic character of the compounds under study.

C.   Surfaces and Interfaces

Surfaces of Heusler compounds have been found not be half-metallic. This is valid irrespectively of the orientation of the surface and it is valid for both the semi-Heusler compounds, as it was shown in the case of NiMnSb (111), (110) and (100) surfaces [93–95], and the full-Heuslers like Co_2MnSn [129]. The loss of half-metallicity is due to surface states pinned exactly at the Fermi level. A similar situation occurs in the case of interfaces with semiconductors [96, 97] where also interface states appear within the minority-spin energy gap. An interesting case occurs at interfaces of full-Heusler compounds containing Cr. The large enhancement of the Cr moment at the interface between a CrAl-terminated $Co_2CrAl(001)$ spacer and the InP(001) semiconductor weakens the effect of the interface states, resulting in the high value of the spin polarization at the Fermi level calculated in reference [128]. Finally, also the case of interfaces between the full-Heusler compounds and magnetic binary compounds has been studied. In cases where both magnetic spacers contain the same transition metal atoms, like the case of $Co_2MnSi/CoPd$ multilayers, a high degree of spin polarization at the interface is present [130].

X.   SUMMARY AND OUTLOOK

In this review we have given an introduction into the electronic structure and the resulting magnetic properties of half-metallic Heusler alloys, which represent interesting hybrids between metallic ferromagnets and semiconductors. Many unusual features arise from the half-metallicity induced by the gap in the minority band, and therefore the understanding of the gap is of central importance.

For the semi-Heusler alloys like NiMnSb, crystallizing in the $C1_b$ structure, the gap arises from the hybridization between the d-wavefunctions of the lower-valent transition metal atom (*e.g.* Mn) with the d-wavefunctions of the higher-valent transition metal atom (*e.g.* Ni). Thus the d-d hybridization leads to 5 occupied bonding bands, which have a larger Ni and smaller Mn admixture. These states form the valence band, being separated by a band

gap from the conduction band which is formed by five antibonding hybrids with a large Mn d- and a small Ni d-admixture. The role of the sp atoms like Sb is very different. Firstly they are important for the bonding, in particular for the stabilization of the $C1_b$ structure. Secondly the sp atom creates for each spin direction one s and three p bands in the energy region below the d states which by hybridization can accommodate also transition metal electrons, such that $e.g.$ Sb formally acts like a Sb^{3-} and Sn as a Sn^{4-} anion. In this way the effective number of valence d-electrons can be changed by the valence of the sp elements.

Since the minority valence band consist of 9 bands, compounds with 18 valence electrons like CoTiSb have the same density of states for both spin directions and are semiconductors. More general, compounds with a total number of Z_t valence electrons per unit cell are ferromagnets and have an integer total spin moment of $M_t = Z_t - 18$, since $Z_t - 18$ is the number of uncompensated spins. For instance, NiMnSb has 22 valence electrons and therefore a total moment of exactly 4 μ_B. This relation is similar to the well known Slater-Pauling behavior observed for binary transition-metal alloys and allows to classify the half-metallic $C1_b$ Heusler alloys into classes with integer moments between 0 and 5 μ_B. The maximum moment of 5 μ_B is difficult to achieve, since it requires that all majority d-sates are occupied.

In the case of the full-Heusler alloys like Co_2MnGe, there are, in addition to the Co-Mn bonding and antibonding d-hybrids, also Co states which cannot hybridize with both the Mn and the Ge atoms and are exclusively localized at the two Co sublattices. Thus in addition to the 5 Co-Mn bonding and 5 Co-Mn antibonding bands, there exist 5 such "non-bonding" bands which are only splitted-up by the weaker Co-Co hybridization into 3 occupied d states of t_{1u} symmetry and 2 unoccupied e_u states, which are located just below and just above the Fermi level such that the indirect gap in these materials is smaller than in the semi-Heuslers. Due to the additional 3 occupied t_{1u} cobalt bands, the full-Heusler alloys have 12 occupied minority bands instead of 9 in the case of the semi-Heusler compounds and their relation for the total spin magnetic moment becomes $M_t = Z_t - 24$. Thus systems like Fe_2VAl with 24 valence electrons are semiconductors, Co_2VAl (26 valence electrons) has a total spin moment of 2 μ_B, Co_2CrAl 3 μ_B, Co_2MnAl 4 μ_B and finally Co_2MnSi which has 29 valence electrons has a total spin moment of 5 μ_B. The maximal total spin moment for these alloys is 7 μ_B, but as has been shown even the 6 μ_B are difficult to be achieved. Special cases of half-metallic full-Heuslers are the inverse

34

Heuslers, the LiMgPdSn-type Heuslers, the disordered quaternary ones (where at one site there exist in a random way atoms of two different chemical species), the so-called half-metallic antiferromagnets which have 24 valence electrons in the unit cell and thus zero net magnetization and finally the magnetic semiconductors including the Heusler compounds showing spin-gapless semiconducting behavior.

The existence of the minority gap is central for any application of half-metals in spintronics, and thus it is of great importance to understand and control all mechanisms that can destroy the gap. The spin-orbit interaction couples the two spin-bands and induces states in the gap; however this effect is weak and the spinpolarization remains in most cases as high as ∼99 % [255]. There are, secondly, excitation effects leading to states in the gap. In the simplest approach one can consider in the adiabatic approximation "static spin waves", which are superpositions of spin-up and spin-down states. At higher temperatures spin-waves excitations will smear out the gap [256, 257]. These excitations drive the system to the paramagnetic state above the Curie temperature. At low temperatures the interaction of the electrons with magnons leads to non-quasiparticle excitations in the minority gap above the Fermi level [258]. Note that spin wave excitations lead to new states in the gap above and below the Fermi level, whereas at low temperatures the non-quasiparticle states introduce only additional states at and above E_{F}. Thirdly and most importantly several kind of defects are expected to lead to states in the gap as discussed above [259].

[1] I. Žutić, J. Fabian, and S. Das Sarma: Rev. Mod. Phys. **76**, 323 (2004).

[2] A. Hirohata and K. Takanashi: J. Phys. D: Appl. Phys. **47**, 193001 (2014).

[3] S.A. Wolf, D. D. Awschalom, R.A. Buhrman, J.M. Daughton, S. von Molnár, M.L. Roukes, A.Y. Chtchelkanova, and D.M. Treger: Science **294**, 1488 (2001).

[4] G.A. Prinz: Science **282**, 1660 (1998).

[5] G.A. Prinz: J. Magn. Magn. Mater. **200**, 57 (1999).

[6] J. de Boeck, W. van Roy, J. Das, V. Motsnyi, Z. Liu, L. Lagae, H. Boeve, K. Dessein, and G. Borghs: Semicond. Sci. Tech. **17**, 342 (2002).

[7] J. de Boeck, W. van Roy, V. Motsnyi, Z. Liu, K. Dessein, and G. Borghs: Thin Solid Films **412**, 3 (2002).

[8] M. Bowen, A. Barthélèmy, M. Bibes, E. Jacquet, J. P. Contour, A. Fert, D. Wortmann, and S. Blügel: J. Phys.: Condens. Matter **17**, L407 (2005).

[9] F. Heusler: Verh. Dtsch. Phys. Ges. **12**, 219 (1903).

[10] P.J. Webster and K.R.A. Ziebeck. In: *Alloys and Compounds of d-Elements with Main Group Elements. Part 2.*, Landolt-Börnstein, New Series, Group III, vol 19c, ed by H.R.J. Wijn, (Springer, Berlin 1988) pp 75–184.

[11] K.R.A. Ziebeck and K.-U. Neumann. In: *Magnetic Properties of Metals*, Landolt-Börnstein, New Series, Group III, vol 32/c, ed by H.R.J. Wijn, (Springer, Berlin 2001) pp 64–414.

[12] J. Pierre, R.V. Skolozdra, J. Tobola, S. Kaprzyk, C. Hordequin, M.A. Kouacou, I. Karla, R. Currat, and E. Lelièvre-Berna: J. Alloys Comp. **262-263**, 101 (1997).

[13] J. Tobola, J. Pierre, S. Kaprzyk, R.V. Skolozdra, and M.A. Kouacou: J. Phys.: Condens. Matter **10**, 1013 (1998).

[14] J. Tobola and J. Pierre: J. Alloys Comp. **296**, 243 (2000).

[15] J. Tobola, S. Kaprzyk, and P. Pecheur: Phys. St. Sol. (b) **236**, 531 (2003).

[16] M. Gillessen and R. Dronskowski: J. Comput. Chem. **30**, 1290 (2009).

[17] M. Gillessen and R. Dronskowski: J. Comput. Chem. **31**, 612 (2010).

[18] K. Watanabe: Trans. Jpn. Inst. Met. **17**, 220 (1976).

[19] R.A. de Groot. F.M. Mueller, P.G. van Engen, and K.H.J. Buschow: Phys. Rev. Lett. **50**, 2024 (1983).

[20] I. Galanakis, P.H. Dederichs, and N. Papanikolaou: Phys. Rev. B **66**, 134428 (2002).

[21] I. Galanakis, P.H. Dederichs, and N. Papanikolaou: Phys. Rev. B **66**, 174429 (2002).

[22] I. Galanakis: J. Phys.: Condens. Matter **16**, 3089 (2004).

[23] M. Zhang, X. Dai, H. Hu, G. Liu, Y. Cui, Z. Liu, J. Chen, J. Wang, and G. Wu: J. Phys: Condens. Matter **15**, 7891 (2003).

[24] M. Zhang, Z. Liu, H. Hu, G. Liu, Y. Cui, G. Wu, E. Brück, F.R. de Boer, and Y. Li : J. Appl. Phys. **95**, 7219 (2004).

[25] R.J. Soulen Jr., J.M. Byers, M.S. Osofsky, B. Nadgorny, T. Ambrose, S.F. Cheng, P.R. Broussard, C.T. Tanaka, J. Nowak, J.S. Moodera, A. Barry, and J.M.D. Coey: Science **282**, 85 (1998).

[26] H. Kato, T. Okuda, Y. Okimoto, Y. Tomioka, K. Oikawa, T. Kamiyama, and Y. Tokura: Phys. Rev. B **69**, 184412 (2004).

[27] T. Shishidou, A.J. Freeman, and R. Asahi: Phys. Rev. B **64**, 180401 (2001).

[28] I. Galanakis: Phys. Rev. B **66**, 012406 (2002).

[29] I. Galanakis and Ph. Mavropoulos: Phys. Rev. B **67**, 104417 (2003).

[30] Ph. Mavropoulos and I. Galanakis: J. Phys.: Condens. Matter **16**, 4261 (2004).

[31] S. Sanvito and N.A. Hill: Phys. Rev. B **62**, 15553 (2000).

[32] A. Continenza, S. Picozzi, W.T. Geng, and A.J. Freeman: Phys. Rev. B **64**, 085204 (2001).

[33] B.G. Liu: Phys. Rev. B **67**, 172411 (2003).

[34] B. Sanyal, L. Bergqvist, and O. Eriksson: Phys. Rev. B **68**, 054417 (2003).

[35] W.-H. Xie, B.-G. Liu, and D.G. Pettifor: Phys. Rev. B **68**, 134407 (2003).

[36] W.-H. Xie, B.-G. Liu, and D.G. Pettifor: Phys. Rev. Lett. **91**, 037204 (2003).

[37] Y.Q. Xu, B.-G. Liu, and D.G. Pettifor: Phys. Rev. B **68**, 184435 (2003).

[38] M. Zhang *et al.*: J. Phys: Condens. Matter **15**, 5017 (2003).

[39] C.Y. Fong, M.C. Qian, J.E. Pask, L.H. Yang, and S. Dag: Appl. Phys. Lett. **84**, 239 (2004).

[40] J.E. Pask, L.H. Yang, C.Y. Fong, W.E. Pickett, and S. Dag: Phys. Rev. B **67**, 224420 (2003).

[41] J.-C. Zheng and J.W. Davenport: Phys. Rev. B **69**, 144415 (2004).

[42] H. Akinaga, T. Manago, and M. Shirai: Jpn. J. Appl. Phys. **39**, L1118 (2000).

[43] M. Mizuguchi, H. Akinaga, T. Manago, K. Ono, M. Oshima, and M. Shirai: J. Magn. Magn. Mater. **239**, 269 (2002).

[44] M. Mizuguchi, H. Akinaga, T. Manago, K. Ono, M. Oshima, M. Shirai, M. Yuri, H.J. Lin, H.H. Hsieh, and C.T. Chen: J. Appl. Phys. **91**, 7917 (2002).

[45] M. Mizuguchi, M.K. Ono, M. Oshima, J. Okabayashi, H. Akinaga, T. Manago, and M. Shirai: Surf. Rev. Lett. **9**, 331 (2002).

[46] M. Nagao, M. Shirai, and Y. Miura: J. Appl. Phys. **95**, 6518 (2004).

[47] K. Ono, J. Okabayashi, M. Mizuguchi, M. Oshima, A. Fujimori, and H. Akinaga: J. Appl. Phys. **91**, 8088 (2002).

[48] M. Shirai: Physica E **10**, 143 (2001).

[49] M. Shirai: J. Appl. Phys. **93**, 6844 (2003).

[50] J.H. Zhao, F. Matsukura, K. Takamura, E. Abe, D. Chiba, and H. Ohno: Appl. Phys. Lett. **79**, 2776 (2001).

[51] J.H. Zhao, F. Matsukura, K. Takamura, E. Abe, D. Chiba, Y. Ohno, K. Ohtani, and H. Ohno: Mat. Sci. Semicond. Proc. **6**, 507 (2003).

[52] M. Horne, P. Strange, W.M. Temmerman, Z. Szotek, A. Svane, and H. Winter: J. Phys.: Condens. Matter **16**, 5061 (2004).

[53] A. Stroppa, S. Picozzi, A. Continenza, and A.J. Freeman: Phys. Rev. B **68**, 155203 (2003).

[54] H. Akai: Phys. Rev. Lett. **81**, 3002 (1998).

[55] K. Kusakabe, M. Geshi, H. Tsukamoto, and N. Suzuki: J. Phys.:Condens. Matter **16**, S5639 (2004).

[56] J.-H. Park, E. Vescovo, H.-J. Kim, C. Kwon, R. Ramesh, and T. Venkatesan: Nature **392**, 794 (1998).

[57] S. Datta and B. Das: Appl. Phys. Lett. **56**, 665 (1990).

[58] K.A. Kilian and R.H. Victora: J. Appl. Phys. **87**, 7064 (2000).

[59] C.T. Tanaka, J. Nowak, and J.S. Moodera: J. Appl. Phys. **86**, 6239 (1999).

[60] J.A. Caballero, Y.D. Park, J.R. Childress, J. Bass, W.-C. Chiang, A.C. Reilly, W.P. Pratt Jr., and F. Petroff: J. Vac. Sci. Technol. A **16**, 1801 (1998).

[61] C. Hordequin, J.P. Nozières, and J. Pierre: J. Magn. Magn. Mater. **183**, 225 (1998).

[62] M.M. Kirillova, A.A. Makhnev, E.I. Shreder, V.P. Dyakina, and N.B. Gorina: Phys. Stat. Sol. (b) **187**, 231 (1995)

[63] K.E.H.M. Hanssen and P.E. Mijnarends: Phys. Rev. B **34**, 5009 (1986).

[64] K.E.H.M. Hanssen, P.E. Mijnarends, L.P.L.M. Rabou, and K.H.J. Buschow: Phys. Rev. B **42**, 1533 (1990)

[65] W. van Roy, M. Wojcik, E. Jdryka, S. Nadolski, D. Jalabert, B. Brijs, G. Borghs, and J. De Boeck: Appl. Phys. Lett. **83**, 4214 (2003).

[66] W. van Roy, J. de Boeck, B. Brijs, and G. Borghs: Appl. Phys. Lett. **77**, 4190 (2000).

[67] J.-P. Schlomka, M. Tolan, and W. Press: Appl. Phys. Lett. **76**, 2005 (2000).

[68] P. Bach, C. Rüster, C. Gould, C.R. Becker, G. Schmidt, and L.W. Molenkamp: J. Cryst. Growth **251**, 323 (2003).

[69] P. Bach, A.S. Bader, C. Rüster, C. Gould, C.R. Becker, G. Schmidt, L.W. Molenkamp, W. Weigand, C. Kumpf, E. Umbach, R. Urban, G. Woltersdorf, and B. Heinrich: Appl. Phys. Lett. **83**, 521 (2003).

[70] J. Giapintzakis, C. Grigorescu, A. Klini, A. Manousaki, V. Zorba, J. Androulakis, Z. Viskadourakis, and C. Fotakis: Appl. Surf. Sci. **197**, 421 (2002).

[71] J. Giapintzakis, C. Grigorescu, A. Klini, A. Manousaki, V. Zorba, J. Androulakis, Z.

Viskadourakis, and C. Fotakis: Appl. Phys. Lett. **80**, 2716 (2002).

[72] C.E.A. Grigorescu, S.A. Manea, M. Mitrea, O. Monnereau, R. Rotonier, L. Tortet, R. Keschawarz, J. Giapintzakis, A. Klini, V. Zorba, J. Androulakis, and C. Fotakis: Appl. Surf. Sci. **212**, 78 (2003).

[73] S. Gardelis, J. Androulaki, P. Migiakis, J. Giapintzakis, S.K. Clowes, Y. Bugoslavsky, W.R. Branford, Y. Miyoshi, and L.F. Cohen: J. Appl. Phys. textbf95, 8063 (2004).

[74] F.B. Mancoff, B.M. Clemens, E.J. Singley, and D.N. Basov: Phys. Rev. B **60**, R12 565 (1999).

[75] W. Zhu, B. Sinkovic, E. Vescovo, C. Tanaka, and J.S. Moodera: Phys. Rev. B **64**, R060403 (2001).

[76] G.L. Bona, F. Meier, M. Taborelli, E. Bucher, and P.H. Schmidt: Sol. St. Commun. **56**, 391 (1985).

[77] S.K. Clowes, Y. Mioyoshi, Y. Bugoslavsky, W.R. Branford, C. Grigorescu, S.A. Manea, O. Monnereau, and L.F. Cohen: Phys. Rev. B **69**, 214425 (2004).

[78] J.A. Caballero, A.C. Reilly, Y. Hao, J. Bass, W.P. Pratt, F. Petroff, and J.R. Childress: J. Magn. Magn. Mat. **198-199**, 55 (1999).

[79] R. Kabani, M. Terada, A. Roshko, and J.S. Moodera: J. Appl. Phys. **67**, 4898 (1990).

[80] C.T. Tanaka, J. Nowak, and J.S. Moodera: J. Appl. Phys. **81**, 5515 (1997).

[81] A. N. Caruso, C. N. Borca, D. Ristoiu, J. P. Nozieres and P. A. Dowben: Surf. Sci. **525**, L109 (2003).

[82] D. Ristoiu, J.P. Nozières, C.N. Borca, T. Komesu, H.-K. Jeong, and P.A. Dowben: Europhys. Lett. **49**, 624 (2000).

[83] D. Ristoiu, J.P. Nozières, C.N. Borca, B. Borca, and P.A. Dowben: Appl. Phys. Lett. **76**, 2349 (2000).

[84] T. Komesu, C.N. Borca, H.-K. Jeong, P.A. Dowben, D. Ristoiu, J.P. Nozières, Sh. Stadler, and Y.U. Idzerda: Phys. Lett. A **273**, 245 (2000).

[85] I. Galanakis, S. Ostanin, M. Alouani, H. Dreyssé, and J.M. Wills: Phys. Rev. B **61**, 4093 (2000).

[86] E. Kulatov and I.I. Mazin: J. Phys.: Condens. Matter **2**, 343 (1990).

[87] S.V. Halilov and E.T. Kulatov: J. Phys.: Condens. Matter **3**, 6363 (1991).

[88] X. Wang, V.P. Antropov, and B.N. Harmon: IEEE Trans. Magn. **30**, 4458 (1994).

[89] S.J. Youn and B.I. Min: Phys. Rev. B **51**, 10436 (1995).

[90] V.N. Antonov, P.M. Oppeneer, A.N. Yaresko, A.Ya. Perlov, and T. Kraft: Phys. Rev. B **56**, 13012 (1997).

[91] P. Larson, S.D. Mahanti, and M.G. Kanatzidis: Phys. Rev. B **62**, 12574 (2000).

[92] D. Orgassa, H. Fujiwara, T.C. Schulthess, and W.H. Butler: Phys. Rev. B **60**, 13237 (1999).

[93] I. Galanakis: J. Phys.:Condens. Matter: **14**, 6329 (2002).

[94] I. Galanakis: J. Magn. Magn. Mater. **288**, 411 (2005).

[95] M. Ležaic, I. Galanakis, G. Bihlmayer, and S. Blügel: J. Phys.:Condens. Matter: **17** 3121 (2005).

[96] I. Galanakis, M. Ležaic, G. Bihlmayer, and S. Blügel: Phys. Rev. B **71**, 214431 (2005).

[97] I. Galanakis, K. Özdoğan, and E. Şaşıoğlu: J. Appl. Phys. **104**, 083916 (2008).

[98] S.J. Jenkins and D.A. King: Surf. Sci. **494**, L793 (2001).

[99] S.J. Jenkins and D.A. King: Surf. Sci. **501**, L185 (2002).

[100] G.A. Wijs and R.A. de Groot: Phys. Rev. B **64**, *R*020402 (2001).

[101] A. Debernardi, M. Peressi, and A. Baldereschi: Mat. Sci. Eng. C-Bio S **23**, 743 (2003).

[102] J. Kübler: Phys. Rev. B **67**, 220403 (2003).

[103] I. Galanakis, E. Şaşıoğlu, and K. Özdoğan: Phys. Rev. B **77**, 214417 (2008).

[104] K. Özdoğan, E. Şaşıoğlu, and I. Galanakis: J. Phys. D: Appl. Phys. **42**, 085003 (2009).

[105] P.J. Webster: J. Phys. Chem. Solids **32**, 1221 (1971).

[106] K.R.A. Ziebeck and P.J. Webster: J. Phys. Chem. Solids **35**, 1 (1974).

[107] J.C. Suits: Phys. Rev. B **14**, 4131 (1976).

[108] J. Kübler, A.R. Williams, and C.B. Sommers: Phys. Rev. B **28**, 1745 (1983).

[109] S. Ishida, S. Akazawa, Y. Kubo, and J. Ishida: J. Phys. F: Met. Phys. **12**, 1111 (1982).

[110] S. Ishida, S. Fujii, S. Kashiwagi, and S. Asano: J. Phys. Soc. Jpn. **64**, 2152 (1995).

[111] S. Fujii, S. Sugimura, S. Ishida, and S. Asano: J. Phys.: Condens. Matter **2**, 8583 (1990).

[112] S. Fujii, S. Asano, and S. Ishida: J. Phys. Soc. Jpn. **64**, 185 (1995).

[113] P.J. Brown, K.U. Neumann, P.J. Webster, and K.R.A. Ziebeck: J. Phys.: Condens. Matter **12**, 1827 (2000).

[114] F.Y. Yang, C.H. Shang, C.L. Chien, T. Ambrose, J.J. Krebs, G.A. Prinz, V.I. Nikitenko, V.S. Gornakov, A.J. Shapiro, and R.D. Shull: Phys. Rev. B **65**, 174410 (2002).

[115] T. Ambrose, J.J. Krebs, and G.A. Prinz: Appl. Phys. Lett. **76**, 3280 (2000).

[116] T. Ambrose, J.J. Krebs, and G.A. Prinz: J. Appl. Phys. **87**, 5463 (2000).

[117] T. Ambrose, J.J. Krebs, and G.A. Prinz: J. Appl. Phys. **89**, 7522 (2001).

[118] M.P. Raphael, B. Ravel, M.A. Willard, S.F. Cheng, B.N. Das, R.M. Stroud, K.M. Bussmann, J.H. Claassen, and V.G. Harris: Appl. Phys. Lett. **70**, 4396 (2001).

[119] M.P. Raphael, B. Ravel, Q. Huang, M.A. Willard, S.F. Cheng, B.N. Das, R.M. Stroud, K.M. Bussmann, J.H. Claassen, and V.G. Harris: Phys. Rev. B **66**, 104429 (2002).

[120] B. Ravel, M.P. Raphael, V.G. Harris, and Q. Huang: Phys. Rev. B **65**, 184431 (2002).

[121] L. Ritchie, G. Xiao, Y. Ji, T.Y. Chen, C.L. Chien, M. Chang, C. Chen, Z. Liu, G.Wu, and X.X. Zhang: Phys. Rev. B **68**, 104430 (2003).

[122] Y.J. Chen, D. Basiaga, J.R. O'Brien, and D. Heiman: Appl. Phys. Lett. **84**, 4301 (2004).

[123] U. Geiersbach, A. Bergmann, and K. Westerholt: J. Magn. Magn. Mater. **240**, 546 (2002).

[124] U. Geiersbach, A. Bergmann, and K. Westerholt: Thin Solid Films **425**, 225 (2003).

[125] K. Westerholt, U. Geirsbach, and A. Bergmann: J. Magn. Magn. Mater. **257**, 239 (2003).

[126] S. Picozzi, A. Continenza, and A.J. Freeman: J. Appl. Phys. **94**, 4723 (2003).

[127] S. Picozzi, A. Continenza, and A.J. Freeman: J. Phys. Chem. Solids **64**, 1697 (2003).

[128] I. Galanakis: J. Phys.:Condens. Matter: **16**, 8007 (2004).

[129] I. Galanakis: J. Comp. Theor. Nanosci. **7**, 474 (2010).

[130] I. Galanakis: J. Magn. Magn. Mater. **377**, 291 (2015).

[131] E. Şaşıoğlu, L.M. Sandratskii, P. Bruno, and I. Galanakis: Phys. Rev. B **72**, 184415 (2005).

[132] I. Galanakis and E. Şaşıoğlu: J. Appl. Phys. **109**, 113912 (2011).

[133] K. Özdoğan and I. Galanakis: J. Appl. Phys. **110**, 076101 (2011).

[134] I. Galanakis, K. Özdoğan, B. Aktaş, and E. Şaşıoğlu: Appl. Phys. Lett. **89**, 042502 (2006).

[135] K. Özdoğan, B. Aktaş, E. Şaşıoğlu, and I. Galanakis: Phys. Rev. B **74**, 172412 (2007).

[136] K. Özdoğan, E. Şaşıoğlu, and I. Galanakis: Phys. St. Sol. (RRL) **1**, 184 (2007).

[137] I. Galanakis, K. Özdoğan, E. Şaşıoğlu, and S. Blügel: J. Appl. Phys. **116**, 033903 (2014).

[138] I. Galanakis, E. Şaşıoğlu, K. Özdoğan, and S. Blügel: hys. Rev. B **90**, 064408 (2014).

[139] K. Özdoğan, I. Galanakis, E. Şaşıoğlu, and B. Aktaş: Phys. St. Sol. (RRL) **1**, 95 (2007).

[140] K. Özdoğan, I. Galanakis, E. Şaşıoğlu, and B. Aktaş: Sol. St. Commun. **142**, 492 (2007).

[141] S. Kämmerer, A. Thomas, A. Hütten, and G. Reiss: Appl. Phys. Lett. **85**, 79 (2004).

[142] J. Schmalhorst, S. Km̈merer, M. Sacher, G. Reiss, A. Hütten, and A. Scholl: Phys. Rev. B **70**, 024426 (2004).

[143] K. Inomata, S. Okamura, R. Goto, and N. Tezuka: Jpn. J. Appl. Phys. **42**, L419 (2003).

[144] K. Inomata, N. Tezuka, S. Okamura, H. Kurebayashi, and H. Hirohata: J. Appl. Phys. **95**, 7234 (2004).

[145] S.H. Vosko, L. Wilk, and N. Nusair: Can. J. Phys. **58**, 1200 (1980).

[146] P, Hohenberg and W. Kohn: Phys. Rev. **136**, B864 (1964).

[147] W. Kohn and L.J. Sham: Phys. Rev. **140**, A1133 (1965).

[148] R. Zeller, P.H. Dederichs, B. Újfalussy, L. Szunyogh, and P. Weinberger: Phys. Rev. B **52**, 8807 (1995).

[149] N. Papanikolaou, R. Zeller, and P.H. Dederichs: J. Phys.: Condens. Matter **14**, 2799 (2002).

[150] M.V. Yablonskikh, V.I. Grebennikov, Yu.M. Yarmoshenko, E.Z. Kurmaev, S.M. Butorin, L.-C. Duda, C. Såthe, T. Kämbre, M. Magnuson, J. Nordgren, S. Plogmann, and M. Neumann: Solid State Commun. **117**, 79 (2001).

[151] M.V. Yablonskikh, Yu.M. Yarmoshenko, V.I. Grebennikov, E.Z. Kurmaev, S.M. Butorin, L.-C. Duda, J. Nordgren, S. Plogmann, and M. Neumann: Phys. Rev. B **63**, 235117 (2001).

[152] R.A. de Groot, A.M. van der Kraan, and K.H.J. Buschow: J. Magn. Magn. Mater. **61**, 330 (1986).

[153] L. Hedin and S. Lundqvist, In: Solid State Physics, vol 23, ed by F. Seitz, D. Turnbull, and H. Ehrenreich, (Academic Press, New York and London 1969) pp 1-181.

[154] B. R. K. Nanda and I. Dasgupta: J. Phys.: Condens. Matter **15**, 7307 (2003).

[155] D. Jung, H.-J. Koo, and M.-H. Whangbo: J. Mol. Struct. (Theochem) **527**, 113 (2000).

[156] J. C. Slater, Phys. Rev. **49**, 931 (1936).

[157] L. Pauling, Phys. Rev. **54**, 899 (1938).

[158] J. Kübler: Physica B **127**, 257 (1984).

[159] I. Galanakis: Phys. Rev. B **71**, 012413 (2005).

[160] D. Brown, M.D. Crapper, K.H. Bedwell, M.T. Butterfield, S.J. Guilfoyle, A.E.R. Malins, and M. Petty: Phys. Rev. B **57**, 1563 (1998).

[161] R.A. Dunlap and D.F. Jones: Phys. Rev. B **26**, 6013 (1982).

[162] S. Plogmann, T. Schlathölter, J. Braun, M. Neumann, Yu.M. Yarmoshenko, M.V. Yablonskikh, E.I. Shreder, E.Z. Kurmaev, A. Wrona, and A. Ślebarski: Phys. Rev. B **60**, 6428 (1999).

[163] P.G. van Engen, K.H.J. Buschow, and M. Erman: J. Magn. Magn. Mater. **30**, 374 (1983).

[164] W. Pendl Jr., R.N. Saxena, A.W. Carbonari, J. Mestnik Filho, and J. Schaff: J. Phys.: Condens. Matter **8**, 11317 (1996).

[165] Ye Feng, J.Y. Rhee, T.A. Wiener, D.W. Lynch, B.E. Hubbard, A.J. Sievers, D.L. Schlagel, T.A. Lograsson, and L.L. Miller: Phys. Rev. B **63**, 165109 (2001).

[166] C.S. Lue, J.H. Ross Jr., K.D.D. Rathnayaka, D.G. Naugle, S.Y. Wu and W.-H. Li: J. Phys.: Condens. Matter **13**, 1585 (2001).

[167] Y. Nishino, H. Kato, M. Kato, U. Mizutani: Phys. Rev. B **63**, 233303 (2001).

[168] A. Matsushita, T. Naka, Y. Takanao, T. Takeuchi, T. Shishido, and Y. Yamada: Phys. Rev. B **65**, 075204 (2002).

[169] K. Özdoğan, I. Galanakis, E. Şaşıoğlu, and B. Aktaş: J. Phys.: Conden. Matter **18**, 2905 (2006).

[170] H. M. Kandpal, G. H. Fecher, C. Felser, and G. Schönhense: Phys. Rev. B **73**, 094422 (2006).

[171] E. Şaşıoğlu, I. Galanakis, C. Friedrich, and S. Blügel: Phys. Rev. B **88**, 134402 (2013).

[172] C. Tsirogiannis and I. Galanakis: arXiv:1501.00732.

[173] K. Özdoğan and I. Galanakis: J. Magn. Magn. Mater. **321**, L34 (2009).

[174] G.D. Liu, X.F. Dai, H.Y. Liu, J.L. Chen, Y.X. Li, G. Xiao, and G.H. Wu: Phys. Rev. B **77**, 014424 (2008).

[175] M. Meinert, J.-M. Schmalhorst, G. Reiss, J. Phys.: Condens. Matter **23**, 116005 (2011).

[176] H. Luo, Z. Zhu, L. Ma, S. Xu, X. Zhu, C. Jiang, H. Xu, and G. Wu: J. Phys. D: Appl. Phys. **41**, 055010 (2008).

[177] J. Li, H. Chen, Y. Li, Y. Xiao, and Z. Li: J. Appl. Phys. **105**, 083717 (2009).

[178] B. Xu, M. Zhang, and H. Yan: Phys. St. Sol.(b) **248**, 2870 (2011).

[179] M. Pugaczowa-Michalska: Intermetallics **24**, 128 (2012).

[180] N. Kervan and S. Kervan: J. Phys. Chem. Sol. **72**, 1358 (2011).

[181] N. Kervan and S. Kervan: Sol. St. Commun. **151**, 1162 (2011).

[182] N. Kervan and S. Kervan: J. Magn. Magn. Mater. **324**, 645 (2012).

[183] E. Bayar, N. Kervan, and S. Kervan: J. Magn. Magn. Mater. **323**, 2945 (2011).

[184] J. Winterlik, G.H. Fecher, B. Balke, T. Graf, V. Alijani, V. Ksenofontov, C.A. Jenkins, O. Meshcheriakova, C. Felser, G. Liu, S. Ueda, K. Kobayashi, T. Nakamura, and M. Wjcik: Phys. Rev. B **83**, 174448 (2011).

[185] M. Meinert, J.-M. Schmalhorst, C. Klewe, G. Reiss, E. Arenholz, T. Bḧnert, and K. Nielsch:

Phys. Rev. B **84**, 132405 (2011).

[186] P. Klaer, C.A. Jenkins, V. Alijani, J. Winterlik, B. Balke, C. Felser, and H.J. Elmers: Appl. Phys. Lett. **98**, 212510 (2011).

[187] V. Alijani, J. Winterlik, G.H. Fecher, and C. Felser, Appl: Phys. Lett. **99**, 222510 (2012).

[188] H. Luo, W. Zhu, L. Ma, G. Liu, Y. Li, X. Zhu, C. Jiang, H. Xu, and G. Wu: J. Phys. D: Appl. Phys. **42**, 095001 (2009).

[189] I. Galanakis and E. Şaşıoğlu: Appl. Phys. Lett. **99**, 052509 (2011).

[190] S. Skaftouros, K. Özdoğan, E. Şaşıoğlu, and I. Galanakis: Phys. Rev. B **87**, 024420 (2013).

[191] D. Xu, G. Liu, G.H. Fecher, C. Felser, Y. Li, and H. Liu: J. Appl. Phys. **105**, 07E901 (2009).

[192] V. Alijani, J. Winterlik, G.H. Fecher, S.S. Naghavi, and C. Felser: Phys. Rev. B **83**, 184428 (2011).

[193] S. Izadi and Z. Nourbakhsh: J. Supercond. Nov. Magn. **24**, 825 (2011).

[194] G. Gökoğlu: Sol. St. Sci. **14**,1273 (2012).

[195] G.Z. Xu, E.K. Liu, Y. Du, G.J. Li, G.D. Liu, W.H. Wang, and G.H. Wu: Europhys. Lett. **102**, 17007 (2013).

[196] K. Özdoğan, E. Şaşıoğlu, and I. Galanakis: J. Appl. Phys. **113**, 193903 (2013).

[197] K. Özdoğan, B. Aktaş, I. Galanakis, and E. Şaşıoğlu: J. Appl. Phys. **101**, 073910 (2007).

[198] Y. Miura, K. Nagao, and M. Shirai: Phys. Rev. B **69**, 144113 (2004).

[199] Y. Miura, M. Shirai, and K. Nagao: J. Appl. Phys. **95**, 7225 (2004)

[200] K. Özdoğan, E. Şaşıoğlu, and I. Galanakis: J. Appl. Phys. **103**, 023503 (2008).

[201] C. Felser, B. Heitkamp, F. Kronast, D. Schmitz, S. Cramm, H.A. Dürr, H.-J. Elmers, G.H. Fecher, S. Wurmehl, T. Block, D. Valdaitsev, S.A. Nepijko, A. Gloskovskii, G. Jakob, G. Schonhense, and W. Eberhardt: J. Phys.:Condens. Matter **15**, 7019 (2003).

[202] N. Auth, G. Jakob, T. Block, and C. Felser: Phys. Rev. B **68**, 024403 (2003).

[203] H. J. Elmers, G.H. Fecher, D. Valdaitsev, S.A. Nepijko, A. Gloskovskii, G. Jakob, G. Schonhense, S. Wurmehl, T. Block, C. Felser, P.-C. Hsu, W.-L. Tsai, and S. Cramm: Phys. Rev. B **67**, 104412 (2003).

[204] T. Block, C. Felser, G. Jakob, J. Ensling, B. Muhling, P. Gutlich, and R.J. Cava: J. Sol. St. Chem. **176**, 646 (2003).

[205] R. Kelekar and B.M. Klemens: J. Appl. Phys. **96**, 540 (2004).

[206] X. Hu: Advanced Materials **24**, 294 (2012).

[207] S. Wurmehl, H.C. Kandpal, G.H. Fecher, and C. Felser: J. Phys.: Condens. Matter **18**, 6171 (2006).

[208] H. van Leuken and R.A. de Groot: Phys. Rev. Lett. **74**, 1171 (1995).

[209] M. Shaughnessy, C Y. Fong, L. H. Yang, and C. Felser 2011, Preprint arXiv::1108.3651.

[210] E. Şaşıoğlu: Phys. Rev. B **79**, 100406(R) (2009).

[211] B. Balke, G.H. Fecher, J. Winterlik, and C. Felser: Appl. Phys. Lett. **90**, 152504 (2007).

[212] J. Winterlik, B. Balke, G.H. Fecher, C. Felser, M.C.M. Alves, F. Bernardi, and J. Morais: Phys. Rev. B **77**, 054406 (2008).

[213] I. Galanakis, K. Özdoğan, E. Şaşıoğlu, and B. Aktaş: Phys. Rev. B **75**, 172405 (2007).

[214] I. Galanakis, K. Özdoğan, E. Şaşıoğlu, and B. Aktaş: Phys. Status Sol. (a) **205**, 1036 (2008).

[215] I. Galanakis, K. Özdoğan, E. Şaşıoğlu, and B. Aktaş: Phys. Rev. B **75**, 092407 (2007).

[216] H. Luo, L. Ma, Z. Zhu, G. Wu, H. Liu, J. Qu, and Y. Li: Physica B **403**, 1797 (2008).

[217] W.E. Pickett: Phys. Rev. B **57**, 10613 (1998).

[218] J.H. Park, S.K. Kwon, and B.I. Min: Phys. Rev. B **65**, 174401 (2002).

[219] M. Uehara, M. Yamada, and Y. Kimishima: Sol. St. Commun. **129**, 385 (2004).

[220] Y.K. Wang and G.Y. Guo: Phys. Rev. B **73**, 064424 (2006).

[221] V. Pardo and W.E. Pickett: Phys. Rev. B **80**, 054415 (2009).

[222] M. Nakao: Phys. Rev. B **74**, 172404 (2006).

[223] M. Nakao: Phys. Rev. B **77**, 134414 (2008).

[224] H. Akai and M. Ogura: Phys. Rev. Lett. **97**, 026401 (2006).

[225] N.H. Long, M. Ogura, and H. Akai: J. Phys.: Condens. Matter **21**, 064241 (2009).

[226] M. Nakao: Phys. Rev. B **83**, 214404 (2011).

[227] S. Picozzi, A. Continenza, and A.J. Freeman: Phys. Rev. B **69**, 094423 (2004).

[228] H. Kurt, K. Rode, M. Venkatesan, P. Stamenov, and J.M.D. Coey: Phys. Rev. B **83**, 020405(R) (2011).

[229] H. Kurt, K. Rode, M. Venkatesan, P. Stamenov, and J.M.D. Coey: Phys. St. Sol. (b) **248**, 2338 (2011).

[230] Q.F. Li, C.H.Yang, and J.L. Su: Physica B **406**, 3726 (2011).

[231] I. Galanakis, K. Özdoğan, and E. Şaşıoğlu: Phys. Rev. B **86**, 134427 (2012).

[232] S. Tirpanci, E. Şaşıoğlu, and I. Galanakis: J. Appl. Phys. **113**, 043912 (2013).

[233] J.S. Moodera, G.-X. Miao, and T.S. Santos: Phys. Today **63**, 46 (2010).

[234] G.-X. Miao, M. Münzenberg, and J.S. Moodera: Rep. Progr. Phys. **74**, 036501 (2011).

[235] I. Galanakis, K. Özdoğan, and E. Şaşıoğlu: Appl. Phys. Lett. **103**, 142404 (2013).

[236] I. Galanakis, K. Özdoğan, and E. Şaşıoğlu: J. Phys.: Condens. Matter, **26**, 086003 (2014).

[237] Isaak M. Tsidilkovski, in *Electron Spectrum of Gapless Semiconductors*, edited by Klaus von Klitzing, Springer Series in Solid-State Sciences Vol. 116 (Springer, New York, 1996).

[238] X. L. Wang: Phys. Rev. Lett. **100**, 156404 (2008).

[239] X. Wang, G. Peleckis, C. Zhang, H. Kimura, and S. Dou: Adv. Mat. **21**, 2196 (2009).

[240] D.H. Kim, J. Hwang, E. Lee, K.J. Lee, S.M. Choo, M.H. Jung, J. Baik, H.J. Shin, B. Kim, K. Kim, B.I. Min, and J.-S. Kang: Appl. Phys. Lett. **104**, 022411 (2014).

[241] S. Skaftouros, K. Özdoğan, E. Şaşıoğlu, and I. Galanakis: Appl. Phys. Lett. **102**, 022402 (2013).

[242] G.Z. Xu, E.K. Liu, Y. Du, G.J. Li, G.D. Liu, W.H. Wang, and G.H. Wu: Europhys. Lett. **102**, 17007 (2013).

[243] G.Y. Gao and K.-L. Yao: Appl. Phys. Lett. **103**, 232409 (2013).

[244] M. Meinert, J. Schmalhorst, and G. Reiss: J. Phys.: Condens. Matter **23**, 036001 (2011).

[245] S. Ouardi, G.H. Fecher, C. Felser, and J. Kübler: Phys. Rev. Lett. **110**, 100401 (2013).

[246] M.E. Jamer, B.A. Assaf, T. Devakul, and D. Heiman: Appl. Phys. Lett. **103**, 142403 (2013).

[247] M.E. Jamer, B.A. Assaf, G.E. Sterbinsky, D.A. Arena, and D. Heiman: J. Appl. Phys. **116**, 213914 (2014).

[248] G.Z. Xu, Y. Du, X.M. Zhang, H.G. Zhang, E.K. Liu, W.H. Wang, and G.H. Wu: Appl. Phys. Lett. **104**, 242408 (2014).

[249] H.Y. Jia, X.F. Dai, L.Y. Wang, R. Liu, X.T. Wang, P.P. Li, Y.T. Cui, and G.D. Liu: AIP Advances **4**, 047113 (2014).

[250] L. Wollmann, S. Chadov, J. Kübler, and C. Felser: Phys. Rev. B **90**, 214420 (2014).

[251] T. Moriya, Spin Fluctuations in Itinerant Electron Magnetism, Springer Series in Solid-State Sciences No. 56 (Springer, Berlin/Heidelberg, 1985).

[252] I. Galanakis, K. Özdoğan, E. Şaşıoğlu, and S. Blügel: J. Appl. Phys. **115**, 093908 (2014).

[253] Y.J. Zhang, G.J. Li, E.K. Liu, J.L. Chen, W.H. Wang, and G.H. Wu: J. Appl. Phys. **113**, 123901 (2013).

[254] J. Kudrnovský, V. Drchal, and I. Turek: Phys. Rev. B **88**, 014422 (2013).

[255] Ph. Mavropoulos, I. Galanakis, V. Popescu, and P.H.Dederichs: J. Phys.: Condens. Matter

16, S5759 (2004).

[256] P.A. Dowben and R. Skomski: J. Appl. Phys. **93**, 7948 (2003).

[257] P.A. Dowben and R. Skomski: J. Appl. Phys. **95**, 7453 (2004).

[258] L. Chioncel, M.I. Katsnelson, R.A. de Groot, and A.I. Lichtenstein: Phys. Rev. B **68**, 144425 (2003).

[259] I. Galanakis and Ph. Mavropoulos: J. Phys.: Condens. Matter **19**, 315213 (2007).

[260] R. Zeller: J. Phys.: Condens. Matter **16**, 6453 (2004).

[261] K. Koepernik and H. Eschrig: Phys. Rev. B **59**, 1743 (1999).

[262] K. Kopernik, Full Potential Local Orbital Minimum Basis Bandstructure Scheme Users Manual (http://www.fplo.de/download/ doc.pdf).